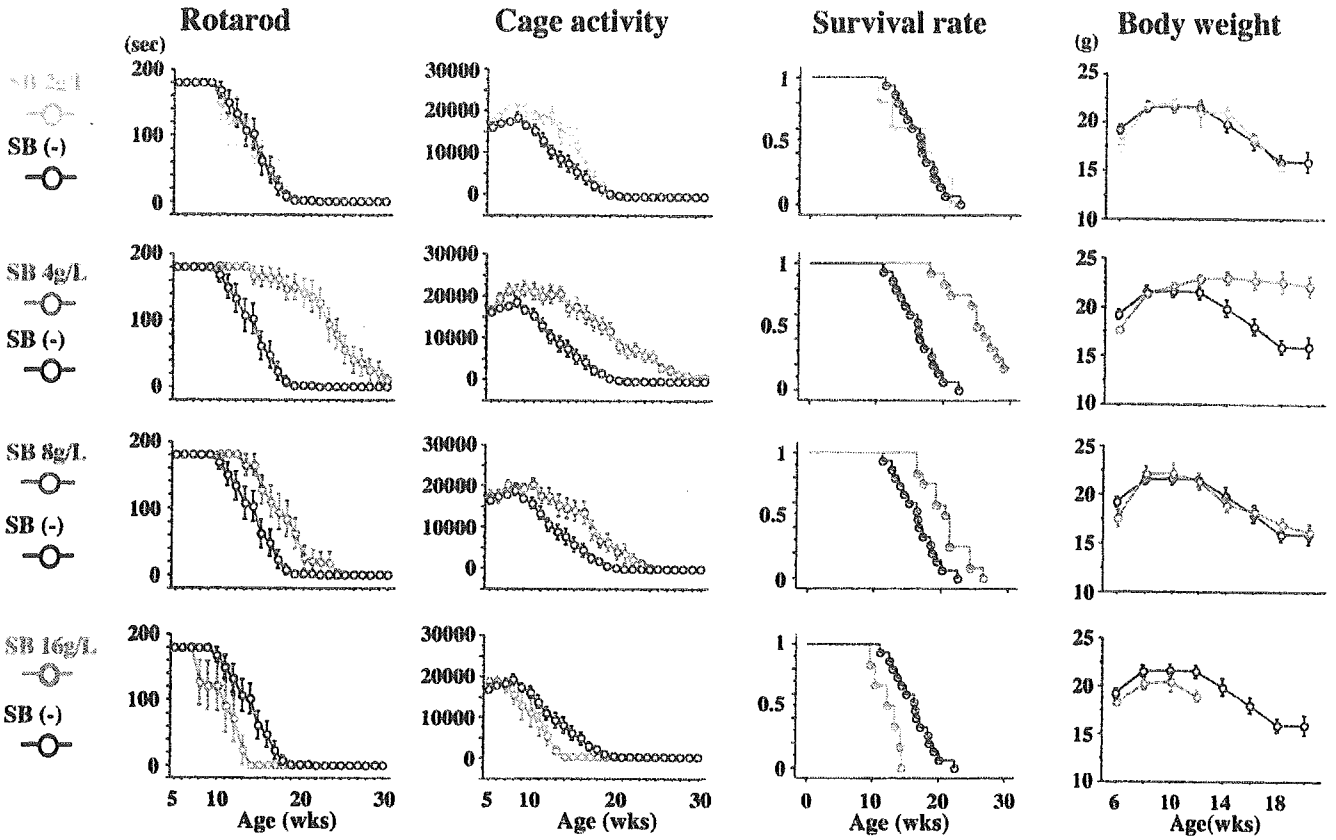

Figure 2. SB ameliorates motor abilities of SBMA Tg mice. Rotarod activity, cage activity, body weight and survival rate (Kaplan–Meier) of Tg mice treated with or without SB ($n = 6$ in SB 2 and 16 g/l, $n = 12$ in SB 4 and 8 g/l, $n = 15$ in water).

anterior horn between SB-treated and non-treated male Tg mice (Fig. 4G–I). Quantitative assessment showed a significant improvement in the mean diameter of muscles (45.7 ± 5.7 μm in the SB-treated Tg mice versus 27.2 ± 12 μm in the non-treated Tg mice, $P = 0.005$), the diameter of large axons in the ventral root (>6 μm) (11.2 ± 0.7 μm in the SB Tg mice versus 9.5 ± 0.4 μm in non-treated Tg mice, $P = 0.02$) and the size of large (>300 μm^2) motor neurons in the lumbar anterior horn (453.0 ± 32.4 μm^2 in the SB-treated Tg mice versus 372.0 ± 38.1 μm^2 in non-treated Tg mice, $P = 0.04$) with oral SB administration at 4 g/l (Fig. 4C, F and I).

SB does not inhibit nuclear localization and aggregation of mutant androgen receptor protein

As we reported earlier (17), nuclear localization and aggregate formation of the mutant AR protein are the major pathways of neuronal dysfunction and phenotypic expression in SBMA. Thus, we examined whether SB administration alters the amount of nuclear-localized mutant AR and the large complex form of mutant AR protein in male Tg mice, using immunohistochemistry with an anti-polyQ antibody, 1C2 and western blotting analysis. As predicted, SB did not decrease the number of neurons and glial cells harboring diffuse nuclear stain with 1C2 and nuclear inclusions in the spinal cord and other central nervous tissues (Fig. 5A). Similarly, SB did not change the 1C2 nuclear staining in visceral organs such as muscle (Fig. 5A). The amount of slowly migrating large complex mass and aggregates of the mutant AR in the spinal cords and muscles (Fig. 5B) as well as in their nuclear fractions (Fig. 5C) was assessed by western blotting with an anti-AR antibody, N-20. SB did not alter the amount of smearing mutant AR protein in the stacking gel. Although CBP was sequestered into the nuclear inclusion in Tg mice, oral SB had no influence on CBP distribution (Fig. 5D).

Oral SB increases histone acetylation level in the central nervous system

It is important to assess the augmentation of histone acetylation in the central nervous system tissue by the oral administration of SB. To determine whether SB increases the acetylation level of histone, we analyzed western blotting of spinal cord homogenate with antibodies against histones H2A, H2B, H3 and H4, and those for acetylated isoforms (Fig. 6A). Without SB treatment, histone acetylation levels are significantly reduced in Tg compared with Wt. Oral SB resulted in a significant increase in the H3 histone acetylation level in male Tg mice at 4 g/l or higher doses, although this effect was not observed at the dose of 2 g/l. The acetylation of histone H3 was also significantly enhanced in Wt mice treated with oral SB (Fig. 6A

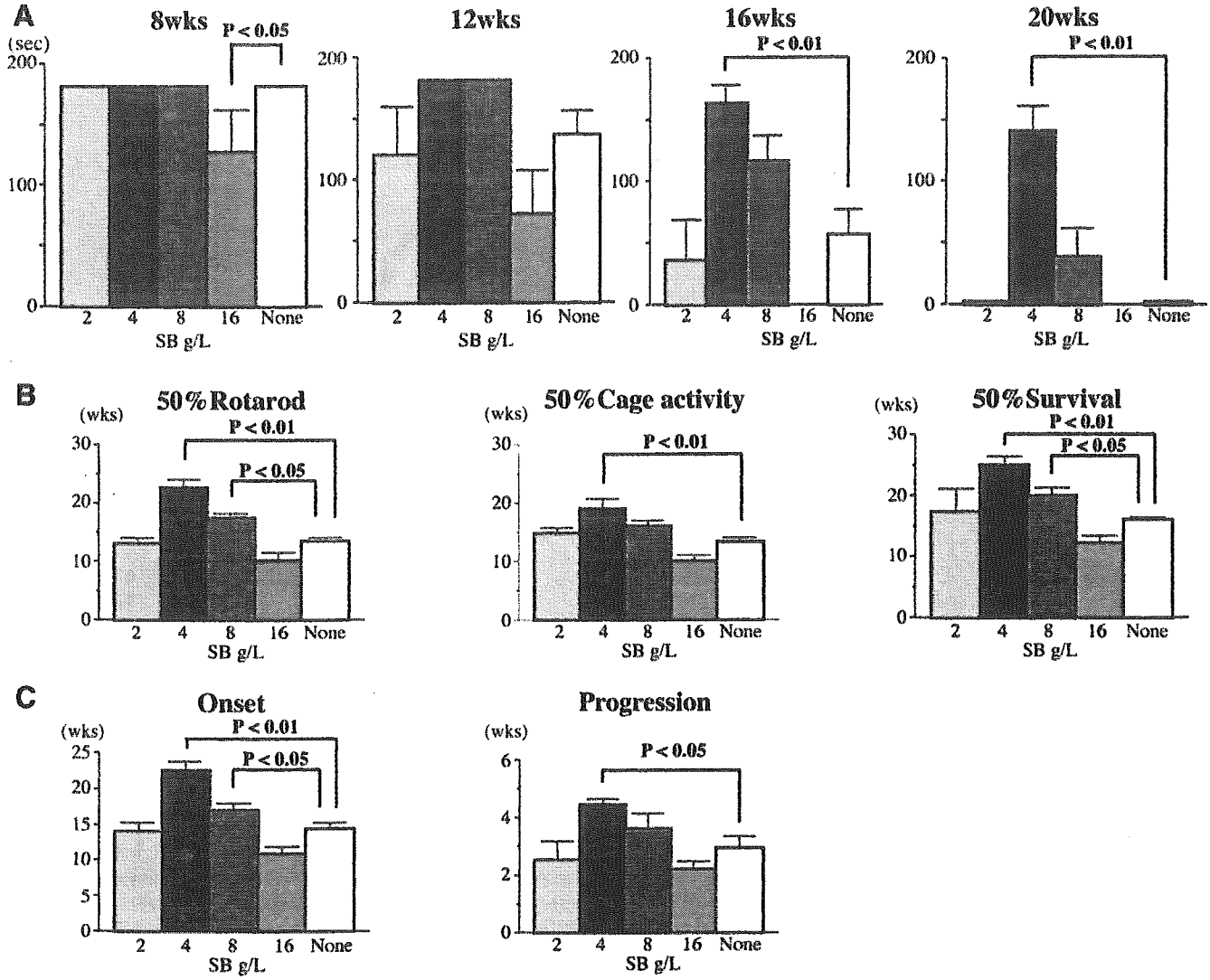

Figure 3. SB exerts therapeutic effects within a narrow dose range. (**A**) Rotarod performance of Tg mice at 8, 12, 16 and 20 weeks of age. The dose effect was bell-shaped at each examined week of age. (**B**) At the dose of 4 g/l, SB prolonged the period during which motor function, assessed by rotarod task and cage activity, declines to 50% of its maximal value, as well as 50% survival. These effects are also observed at 8 g/l, although to a lesser extent than at 4 g/l. (**C**) The onset of rotarod task decline and the period from the onset to death in each treatment group. The symptomatic onset is retarded by SB at 4 or 8 g/l, whereas the progression is slowed only at the dose of 4 g/l. (A, B and C: $n = 6$ in SB 2 and 16 g/l, $n = 12$ in SB 4 and 8 g/l, $n = 15$ in water).

and B). In contrast to H3, acetylation of histones H2A, H2B and H4 was not significantly augmented by oral SB administration at any dose (Fig. 6A). Similar effects were observed in the brain and muscle (data not shown).

Immunohistochemistry with the antibody specific to acetylated H3 demonstrated that the nuclei of the spinal cord motor neurons and glial cells were more densely stained in mice given oral SB than in non-treated mice. The staining intensity was proportional to the oral SB doses (Fig. 6C). The numbers of anti-acetylated histone H3 positive neurons and glia cells were significantly greater in SB-treated Tg mice than in non-treated mice (Fig. 6D).

These observations indicate that SB is capable of crossing the blood–brain barrier and increasing the level of H3 acetylation in the spinal cord and brain, providing the theoretical basis for this SBMA treatment.

DISCUSSION

A growing number of polyQ diseases share salient clinical features including anticipation and selective distribution of pathology, and their symptoms are influenced by the number of CAG repeats in the causative gene (1,2). Although the gene products are unrelated except for the presence of polyQ tract, some nervous tissues, including the spinal anterior horn, brainstem and cerebellum, are preferentially affected in polyQ diseases. NIs detected in these lesions are the pathological hallmark of the disorders. The observations of common phenotypes led to the hypothesis that unifying mechanisms underlie the pathogenesis of polyQ diseases. Transcriptional dysregulation (16,27,28), aggregate formation (29,30), proteolysis of causative protein (31), transglutaminase activation (32) and mitochondrial deficits (33) have been implicated

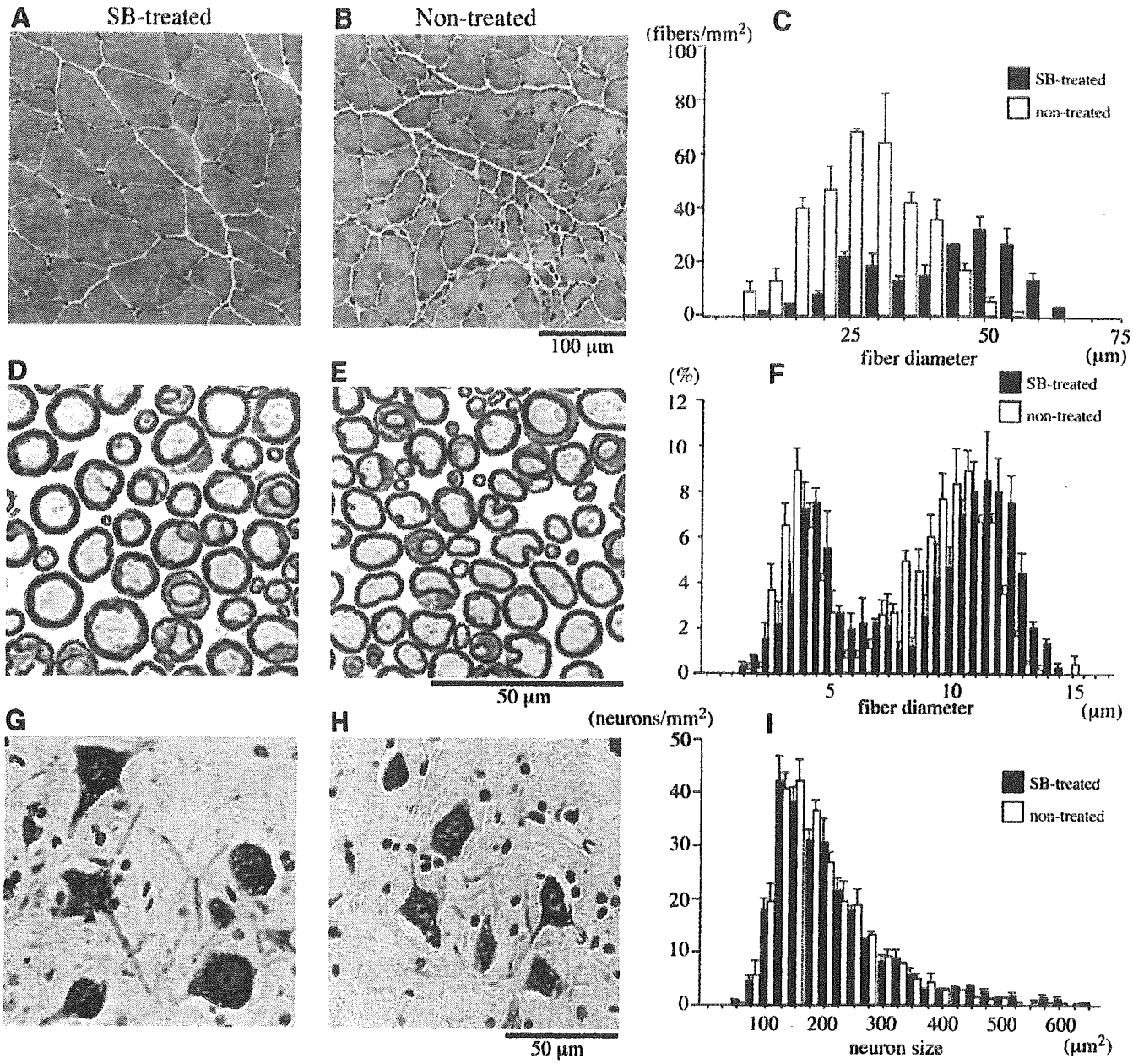

Figure 4. Amelioration of neuropathological findings by SB treatment. (**A**–**C**). Muscle H&E staining (A and B) of the SB-treated and non-treated male Tg mice (12 weeks old), and the histogram of muscle fiber diameter (C, $n = 3$ in each group). (**D**–**F**) Toluidine blue staining of the L5 ventral root of male Tg mice treated with or without SB (D and E), and the histogram of myelinated fiber diameter (F, $n = 3$). (**G**–**I**) Nissl staining of the lumbar anterior horn of Tg mice of each treatment group (G and H), and the histogram of motor neuron size (I, $n = 3$).

in the pathogenesis, and have been expected to be targets of medical intervention. Among these hypotheses, altered transcription appears to be convincing, supported by the fact that most polyQ proteins have been implicated in transcriptional regulation (34).

Gene expression analysis indicates that transcriptional disruption is an early change in the pathogenesis of mouse models of polyQ diseases (35,36). The expression of genes regulated through cAMP-response element-mediated transcription is decreased in HD mouse models (37,38). The transcription co-activators are sequestrated into aggregation, and their function is inhibited by soluble polyQ-containing protein (2). As the HAT activity of CBP is suppressed in cellular models, a decrease in histone acetylation is likely to underlie the neurodegeneration in polyQ diseases. Although this hypothesis has been confirmed *in vitro*, it remains unclear whether the histone acetylation level is decreased in animal models (26,39). The present study demonstrates that the acetylation of nuclear histone is diminished in SBMA Tg mice, suggesting that the HAT activity of CBP is suppressed *in vivo*. The restoration of histone acetylation by HDAC inhibitors has been considered to be of therapeutic

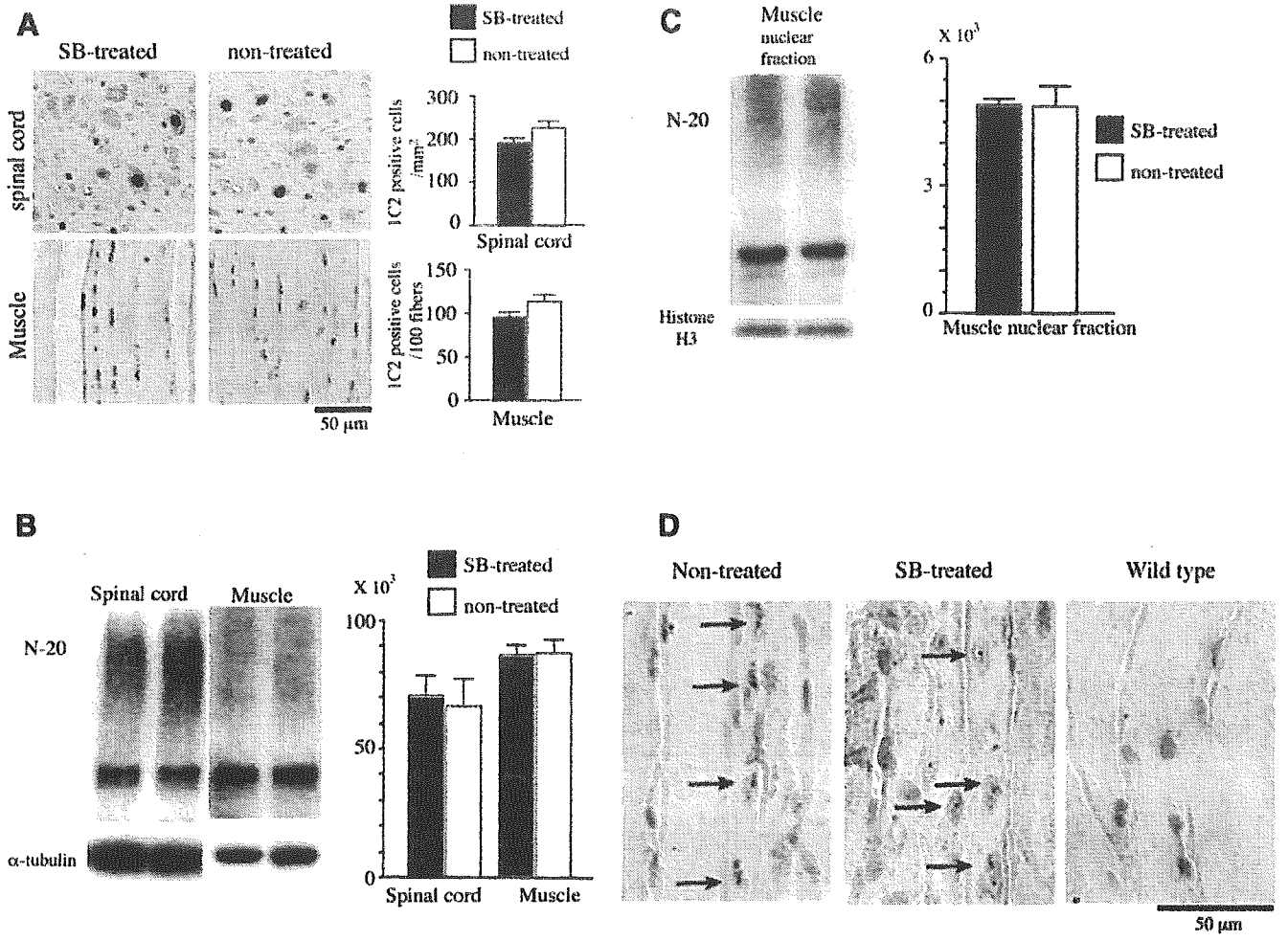

Figure 5. SB does not prevent nuclear accumulation of mutant AR. **(A)** Immunohistochemistry with anti-polyQ antibody of the spinal cord and muscle of Tg mice treated with or without SB (12 weeks old). **(B)** Western blot analysis with an anti-AR antibody, N-20, of total homogenates from the spinal cord and muscle of the SB-treated and non-treated male Tg mice (12 weeks old). Densitometric analysis demonstrated no difference in the amount of smearing mutant AR protein between SB-treated and non-treated Tg mice ($n = 3$, $P = 0.79$ for spinal cord and $P = 0.93$ for muscle). **(C)** Western blot analysis of nuclear fraction from the muscle of male mice with N-20 (12 weeks old). In the densitometric analysis, SB did not reduce the amount of smearing mutant AR in the nuclear fraction ($n = 3$, $P = 0.89$). **(D)** Immunohistochemistry of the muscle demonstrates that CBP is sequestrated into the nuclear inclusion in Tg mice (12 weeks old) regardless of SB treatment.

benefit in polyQ diseases (40). Although HDAC inhibitors mitigate polyQ-induced neurodegeneration in cell and fly models of polyQ diseases (24,25), SAHA is of limited therapeutic benefit in a mouse model of HD owing to its toxicity (26). Based on their ability to regulate transcriptional activity, HDAC inhibitors have also been employed in experimental therapies for malignancies and endocrinological disorders (41). In experimental cancer therapy, as observed in polyQ models, higher doses of HDAC inhibitor are required in animal models than *in vitro*, presumably because of the fast elimination and low bioavailability of these compounds *in vivo*. The cytotoxicity of HDAC inhibitor is considerable, especially in dividing cells, and this needs to be overcome for clinical use. SAHA demonstrated remarkable side effects, including leukopenia, thrombocytopenia, hypotension, acute respiratory distress, renal insufficiency, tumor-related pain and fatigue, in a phase I clinical trial for malignancies (42). Dose-limiting toxicities were neuro-cortical events such as somnolence and confusion in another phase I clinical trial with phenylbutyrate (43).

SB is less potent than SAHA, but has the advantage of less serious toxicity. Our present study demonstrates that oral SB exerts therapeutic effects with subtle side effects when it is used at an appropriate dose. Our results revealed that the most beneficial effects were achieved at the oral SB dose of 4 g/l, whereas the compound was partially effective at the dose of 8 g/l. The acetylation level of histone is increased at these doses, implying that improvement of transcription contributes to the amelioration of symptomatic and histopathological phenotypes. SB caused no amelioration of the pathogenesis at 2 g/l, presumably because it failed to augment histone acetylation.

It is intriguing that Tg mice had lower tolerance to the toxicity of SB than did Wt. The dose of 16 g/l, which did not harm Wt mice, aggravated motor dysfunction in the Tg mice. This appears to result from the adverse effect of SB,

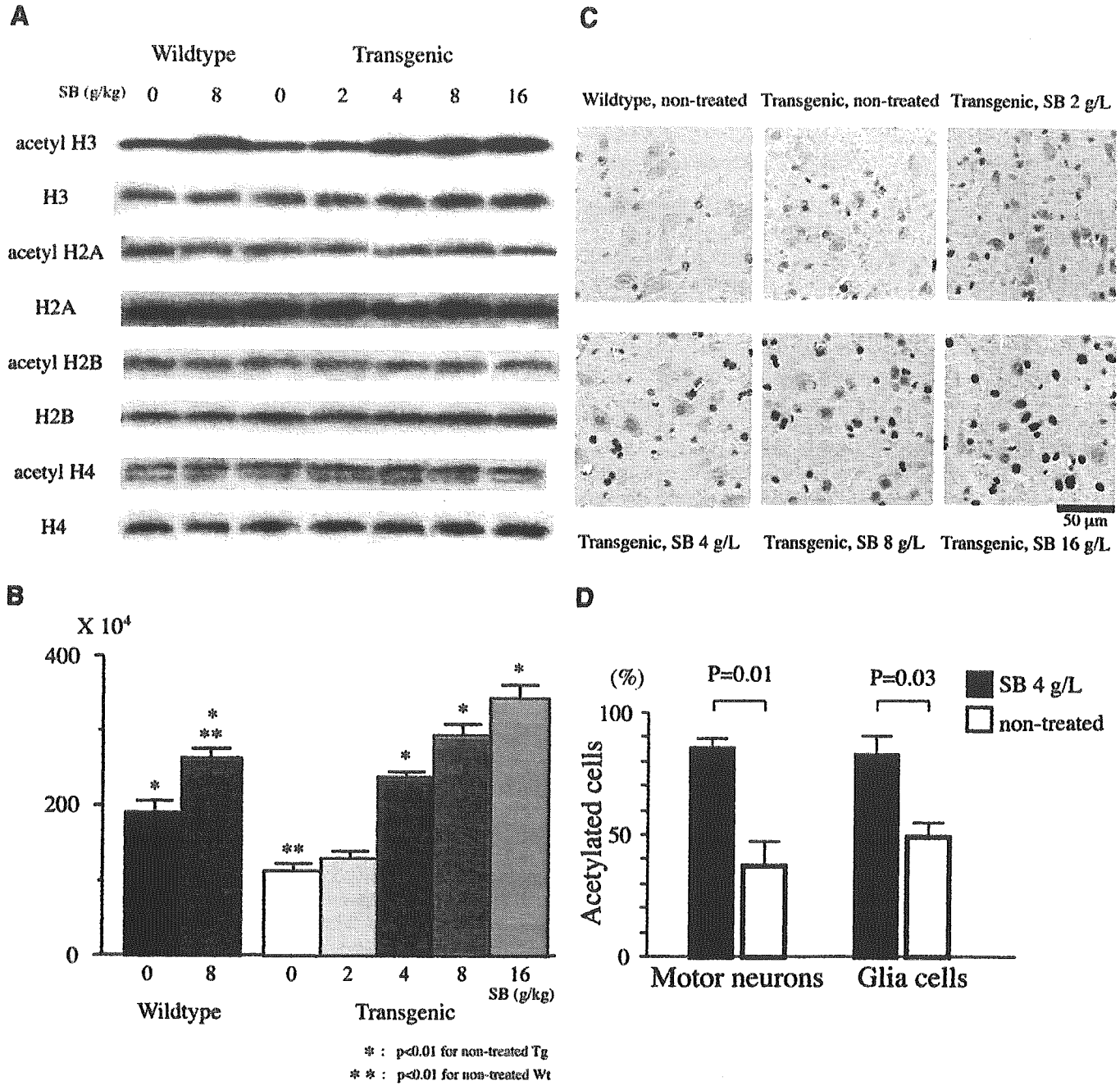

Figure 6. SB induces acetylation of nuclear histone in mice. (**A**) Western blot analysis of the spinal cord of Wt and Tg mice with the antibodies against histones: H3, H4, H2A and H2B. Each blot was reprobed with the antibodies against the acetylated isoform of the histones. (**B**) The acetylation level of histone H3 was quantitated using densitometry ($n = 6$ for each group). (**C**) Immunohistochemistry of the spinal cord of the SB-treated and non-treated Tg mice with antibodies against acetylated H3. (**D**) Densitometric analysis of immunohistochemistry shows that the acetylation level of both neurons and glial cells are upregulated at 4 g/l of SB.

as the histone acetylation level was successfully increased in the central nervous system at this dose. SB induces metabolic acidosis and even death at high doses in mice (44). Immobility, dehydration and exhaustion may lower the threshold for adverse effects of SB in Tg mice. This observation should also be kept in mind during clinical trials.

Intraperitoneal delivery of SB has also been reported to ameliorate neurodegeneration in an HD mouse model (39). This study supports our findings that SB improves the pathogenesis of polyQ diseases at an appropriate dose. Although intraperitoneal administration of SB upregulates acetylation of both histones H3 and H4, the present study demonstrated H3 selectivity of the effect of oral SB treatment. As SB is rapidly eliminated *in vivo* (44), the route of SB administration may influence its effect on histone acetylation as well as its side effects. Alternatively, a higher dose of SB might be

required for H4 acetylation; indeed, the most effective dose of SB in HD mouse study, 1200 mg/kg/day, was higher than that in our analysis, 800–900 mg/kg/day.

We have previously described therapeutic approaches for SBMA using our Tg mouse model (45). Reduction in the testosterone level by castration or leuprorelin administration diminished nuclear-localized mutant AR and markedly prevented phenotypic expression in the male Tg mice (17,18). Overexpression of heat shock protein 70, which is a molecular chaperone refolding mutant protein (46), resulted in acceleration of mutant AR degradation and phenotypic amelioration (19). Although these strategies show therapeutic promise, single therapeutic agents possess limited potential because of their side effects. As suggested for other neurodegenerative diseases (47), combinations of drugs appear to be useful in the attempts of obtaining maximal therapeutic effects and reducing harmful events. Although the exact mechanism remains to be clarified, SB also ameliorates neuromuscular phenotypes of spinal muscular atrophy, which is another lower motor neuron disease arising from a different gene mutation (48). This result might indicate the relatively potent effects of SB on affected lower motor neurons. SB is a promising candidate for combination therapy for SBMA, although its dose should be very carefully determined for clinical use.

MATERIALS AND METHODS

Generation and maintenance of Tg mice and genotyping

Chicken β-actin promoter-driven AR-24Q and AR-97Q constructs were prepared by digestion of pCAGGS vector as described earlier (17,49,50). Genotyping of mice was performed by PCR using mouse tail (17). Tg mice were maintained by crossing to F1 of C57BL/6J and BDF1. We analyzed a symptomatic line #4–6 of this mouse model throughout the present study.

Assessment of motor ability

All animal experiments were performed in accordance with the National Institute of Health Guide for the Care and Use of Laboratory Animals and were approved by the Nagoya University Animal Experiment Committee. Rotarod performance was assessed weekly using an Economex Rotarod (Colombus Instruments, Colombus, OH, USA) as described previously (51). Cage activity was measured weekly, with each mouse in a transparent acrylic cage within a soundproof box as described previously (17).

Administration of SB

Wt and SBMA Tg (AR-97Q #4–6) mice were orally supplied sterile water *ad libitum*. Three mice shared the same drinking water in each cage. SB was administered at a concentration of 2, 4, 8, 16 or 40 g/l in distilled water from 5 weeks of age until the end of analysis. Before the onset of motor symptoms, between the age of 6 and 8 weeks, the approximate daily amount of drinking water was similar for each treatment group of Tg mice; 4.0 ± 0.26, 3.7 ± 0.51, 4.5 ± 0.19, 4.1 ± 0.29 and 4.4 ± 0.15 ml at the dose of 0, 2, 4, 8 and 16 g/l, respectively. There was no difference in the amount of water intake and body weight between Wt and Tg mice in that period.

Immunohistochemistry

An aliquot of 20 ml of 4% paraformaldehyde fixative in 0.1 M phosphate buffer (pH 7.4) was perfused through the left cardiac ventricle of mice (12 weeks old) deeply anesthetized with ketamine–xylazine, the tissues post-fixed in 10% phosphate-buffered formalin and then processed for paraffin embedding. Tissue sections (4 μm thick) were then deparaffinized, dehydrated with alcohol, and then treated for antigen retrieval (17). For the mutant AR immunohistochemical study, the paraffin sections were pretreated with formic acid for 5 min at room temperature. The tissue sections were blocked with normal horse serum (1 : 20) and incubated with mouse anti-expanded polyQ, 1C2 (1 : 10 000, Chemicon, Temecula, CA, USA). The sections were then incubated with biotinylated anti-mouse IgG (1 : 1000, Vector Laboratories, Burlingame, CA, USA). Immune complexes were visualized using streptavidin–horseradish peroxidase (Dako, Glostrup, Denmark) and 3,3′-diaminobenzidine (Dojindo, Kumamoto, Japan) substrate. Sections were counterstained with methyl green. For immunostaining of histone, sections were autoclaved at 121°C for 15 min, and incubated with anti-histone H3 (1 : 100, Upstate Biotechnology, Lake Placid, NY, USA) or anti-acetylated histone H3 (1 : 500, Upstate Biotechnology) antibodies.

The number of 1C2 or anti-acetylated H3-positive cells for one individual mouse was counted using a light microscope with a computer-assisted image analyzer (Luzex FS, Nikon, Tokyo, Japan). Fifty consecutive transverse sections of the thoracic spinal cord were prepared, and 1C2 or anti-acetylated H3-positive cells in the anterior horn on every fifth section were counted as described previously (51,52). For quantitative assessment, 1C2-positive cells in the muscle were calculated from counts of more than 500 fibers in randomly selected areas, and were expressed as the number per 100 muscle fibers.

Muscle histology and morphometric analysis of spinal motor neurons and ventral spinal roots

Cryostat sections of the gastrocnemius muscles (6 μm thick) were air-dried and stained with hematoxylin and eosin (H&E). The muscle fiber diameter was measured in randomly selected areas for three mice of each treatment group (12 weeks old) using a Luzex FS image analyzer (Nireco). To assess the neuronal populations and cross-sectional area of the anterior horn cells, 20 serial 5 μm thick sections from the fifth lumbar spinal cords of three mice of each group (12 weeks old) were prepared. Every other section was stained by the Nissl technique, and all neurons with an obvious nucleolus in the anterior horn were assessed using a Luzex FS image analyzer as described earlier (17). The diameter of myelinated fibers in the ventral spinal roots was measured on the transverse sections stained with toluidine blue, also as described earlier (17).

Western blots

Mice (12 weeks old) were exsanguinated under ketamine–xylazine anesthesia, and their tissues snap-frozen with powdered CO_2 in acetone. Frozen tissue (0.1 g wet weight) was homogenized in 1000 μl of CelLytic-M mammalian cell lysis/extraction reagent (Sigma Chemical, St Louis, MO, USA) with 1 mM phenylmethylsulfonyl fluoride and aprotinin at 6 μg/ml. Homogenates were spun at 2500*g* for 15 min at 4°C. The protein concentration of the supernatant was determined using DC protein assay (Bio-Rad Laboratories, Hercules, CA, USA). Each lane on a 5–20% SDS–PAGE gel was loaded with 200 μg protein for the spinal cord and 80 μg for the muscle from the supernatant fraction, which was transferred to Hybond-P membranes (Amersham Pharmacia Biotech, Buckinghamshire, UK) using 25 mM Tris, 192 mM glycine and 10% methanol as transfer buffer. Kaleidoscope prestained standards were used as size markers (Bio-Rad Laboratories). Proteins were then transferred to Hybond-P membranes (Amersham Pharmacia Biotech), which were subsequently blocked in 5% milk in Tris-buffered saline containing 0.05% Tween-20, and incubated with appropriate primary antibodies using standard techniques. Primary antibodies were used at the following concentrations: anti-histone H3, 1 : 500 (Upstate Biotechnology); anti-acetylated histone H3, 1 : 250 (Upstate Biotechnology); anti-histone H4, 1 : 500 (Upstate Biotechnology); anti-acetylated histone H4, 1 : 200 (Upstate Biotechnology); anti-histone H2A, 1 : 500 (Upstate Biotechnology); anti-acetylated histone H2A, 1 : 200 (Upstate Biotechnology); anti-histone H2B, 1 : 500 (Upstate Biotechnology) and anti-acetylated histone H2B, 1 : 200 (Serotec, Kidlington, UK). Second antibody probing and detection were performed using the ECL + plus kit (Amersham Pharmacia Biotech) as described earlier (17). The signal intensity of the bands smearing from the top of the gel were quantified using the NIH Image program (NIH Image version 1.62). The quantitative data of three independent western blots were expressed as mean ± SD.

Statistical analyses

Data were analyzed using Kaplan–Meier and log-rank test for survival rate in Figure 2, Dunnett test for multiple comparison in Figures 3A–C and 6B and unpaired *t*-test in Figures 4, 5 and 6D from Statview software version 5 (HULINKS, Tokyo, Japan).

ACKNOWLEDGEMENTS

We thank Dr Tamakoshi and Dr Yatsuya for their advice in the statistical analysis. This work was supported by a Center-of-Excellence (COE) grant from the Ministry of Education, Culture, Sports, Science and Technology, Japan, grants from the Ministry of Health, Labor and Welfare, Japan, a grant from the Naito Foundation and a grant from the Kanae Foundation.

REFERENCES

1. Zoghbi, H.Y. and Orr, H.T. (2000) Glutamine repeats and neurodegeneration. *Annu. Rev. Neurosci.*, **23**, 217–247.
2. Ross, C.A. (2002) Polyglutamine pathogenesis: emergence of unifying mechanisms for Huntington's disease and related disorders. *Neuron*, **35**, 819–822.
3. Margolis, R.L. and Ross, C.A. (2002) Expansion explosion: new clues to the pathogenesis of repeat expansion neurodegenerative diseases. *Trends. Mol. Med.*, **7**, 479–482.
4. Kennedy, W.R., Alter, M. and Sung, J.H. (1968) Progressive proximal spinal and bulbar muscular atrophy of late onset. A sex-linked recessive trait. *Neurology*, **18**, 671–680.
5. Sobue, G., Hashizume, Y., Mukai, E., Hirayama, M., Mitsuma, T. and Takahashi, A. (1989) X-linked recessive bulbospinal neuronopathy. A clinicopathological study. *Brain*, **112**, 209–232.
6. Takahashi, A. (2001) Hiroshi Kawahara (1858–1918). *J. Neurol.*, **248**, 241–242.
7. La Spada, A.R., Wilson, E.M., Lubahn, D.B., Harding, A.E. and Fischbeck, K.H. (1991) Androgen receptor gene mutations in X-linked spinal and bulbar muscular atrophy. *Nature*, **352**, 77–79.
8. Tanaka, F., Doyu, M., Ito, Y., Matsumoto, M., Mitsuma, T., Abe, K., Aoki, M., Itoyama, Y., Fischbeck, K.H. and Sobue, G. (1996) Founder effect in spinal and bulbar muscular atrophy (SBMA). *Hum. Mol. Genet.*, **5**, 1253–1257.
9. Tanaka, F., Reeves, M.F., Ito, Y., Matsumoto, M., Li, M., Miwa, S., Inukai, A., Yamamoto, M., Doyu, M., Yoshida, M. *et al.* (1999) Tissue-specific somatic mosaicism in spinal and bulbar muscular atrophy is dependent on CAG-repeat length and androgen receptor–gene expression level. *Am. J. Hum. Genet.*, **65**, 966–973.
10. Doyu, M., Sobue, G., Mukai, E., Kachi, T., Yasuda, T., Mitsuma, T. and Takahashi, A. (1992) Severity of X-linked recessive bulbospinal neuronopathy correlates with size of the tandem CAG repeat in androgen receptor gene. *Ann. Neurol.*, **23**, 707–710.
11. La Spada, A.R., Roling, D.B., Harding, A.E., Warner, C.L., Spiegel, R., Hausmanowa-Petrusewicz, I., Yee, W.C. and Fischbeck, K.H. (1992) Meiotic stability and genotype-phenotype correlation of the trinucleotide repeat in X-linked spinal and bulbar muscular atrophy. *Nat. Genet.*, **2**, 301–304.
12. Igarashi, S., Tanno, Y., Onodera, O., Yamazaki, M., Sato, S., Ishikawa, A., Miyatani, N., Nagashima, M., Ishikawa, Y., Sahashi, K. *et al.* (1992) Strong correlation between the number of CAG repeats in androgen receptor genes and the clinical onset of features of spinal and bulbar muscular atrophy. *Neurology*, **42**, 2300–2302.
13. Li, M., Miwa, S., Kobayashi, Y., Merry, D.E., Tanaka, F., Doyu, M., Hashizume, Y., Fischbeck, K.H. and Sobue, G. (1998) Nuclear inclusions of the androgen receptor protein in spinal and bulbar muscular atrophy. *Ann. Neurol.*, **44**, 249–254.
14. Li, M., Nakagomi, Y., Kobayashi, Y., Merry, D.E., Tanaka, F., Doyu, M., Mitsuma, T., Fischbeck, K.H. and Sobue, G. (1998) Nonneural nuclear inclusions of androgen receptor protein in spinal and bulbar muscular atrophy. *Am. J. Pathol.*, **153**, 695–701.
15. Tobin, A.J. and Signer, E.R. (2000) Huntington's disease: the challenge for cell biologists. *Trends Cell Biol.*, **10**, 531–536.
16. Taylor, J.P., Hardy, J. and Fischbeck, K.H. (2002) Toxic proteins in neurodegenerative disease. *Science*, **296**, 1991–1995.
17. Katsuno, M., Adachi, H., Kume, A., Li, M., Nakagomi, Y., Niwa, H., Sang, C., Kobayashi, Y., Doyu, M. and Sobue, G. (2002) Testosterone reduction prevents phenotypic expression in a transgenic mouse model of spinal and bulbar muscular atrophy. *Neuron*, **35**, 843–854.
18. Katsuno, M., Adachi, H., Doyu, M., Minamiyama, M., Sang, C., Kobayashi, Y., Inukai, A. and Sobue, G. (2003) Leuprorelin rescues polyglutamine-dependent phenotypes in a transgenic mouse model of spinal and bulbar muscular atrophy. *Nat. Med.*, **9**, 768–773.
19. Adachi, H., Katsuno, M., Minamiyama, M., Sang, C., Pagoulatos, G., Angelidis, C., Kusakabe, M., Yoshiki, A., Kobayashi, Y., Doyu, M. *et al.* (2003) Heat shock protein 70 chaperone overexpression ameliorates phenotypes of the spinal and bulbar muscular atrophy transgenic mouse model by reducing nuclear-localized mutant androgen receptor protein. *J. Neurosci.*, **23**, 2203–2211.
20. McCampbell, A., Taylor, J.P., Taye, A.A., Robitschek, J., Li, M., Walcott, J., Merry, D., Chai, Y., Paulson, H., Sobue, G. *et al.* (2000) CREB-binding protein sequestration by expanded polyglutamine. *Hum. Mol. Genet.*, **9**, 2197–2202.
21. Nucifora, F.C. Jr, Sasaki, M., Peters, M.F., Huang, H., Cooper, J.K., Yamada, M., Takahashi, H., Tsuji, S., Troncoso, J., Dawson, V.L. *et al.*

(2001) Interference by huntingtin and atrophin-1 with CBP-mediated transcription leading to cellular toxicity. *Science*, **291**, 2423–2428.
22. Steffan, J.S., Kazantsev, A., Spasic-Boskovic, O., Greenwald, M., Zhu, Y.Z., Gohler, H., Wanker, E.E., Bates, G.P., Housman, D.E. and Thompson, L.M. (2000) The Huntington's disease protein interacts with p53 and CREB-binding protein and represses transcription. *Proc. Natl Acad. Sci. USA*, **97**, 6763–6768.
23. Dunah, A.W., Jeong, H., Griffin, A., Kim, Y.M., Standaert, D.G., Hersch, S.M., Mouradian, M.M., Young, A.B., Tanese, N. and Krainc, D. (2002) Sp1 and TAFII130 transcriptional activity disrupted in early Huntington's disease. *Science*, **296**, 2238–2243.
24. Steffan, J.S., Bodai, L., Pallos, J., Poelman, M., McCampbell, A., Apostol, B.L., Kazantsev, A., Schmidt, E., Zhu, Y.Z., Greenwald, M. *et al.* (2001) Histone deacetylase inhibitors arrest polyglutamine-dependent neurodegeneration in *Drosophila*. *Nature*, **413**, 739–743.
25. McCampbell, A., Taye, A.A., Whitty, L., Penney, E., Steffan, J.S. and Fischbeck, K.H. (2001) Histone deacetylase inhibitors reduce polyglutamine toxicity. *Proc. Natl Acad. Sci. USA*, **98**, 15179–15184.
26. Hockly, E., Richon, V.M., Woodman, B., Smith, D.L., Zhou, X., Rosa, E., Sathasivam, K., Ghazi-Noori, S., Mahal, A., Lowden, P.A. *et al.* (2003) Suberoylanilide hydroxamic acid, a histone deacetylase inhibitor, ameliorates motor deficits in a mouse model of Huntington's disease. *Proc. Natl Acad. Sci. USA*, **100**, 2041–2046.
27. Cha, J.H. (2000) Transcriptional dysregulation in Huntington's disease. *Trends Neurosci.*, **23**, 387–392.
28. Sugars, K.L. and Rubinsztein, D.C. (2003) Transcriptional abnormalities in Huntington disease. *Trends Genet.*, **19**, 233–238.
29. Bates, G. (2003) Huntingtin aggregation and toxicity in Huntington's disease. *Lancet*, **361**, 1642–1644.
30. Sanchez, I., Mahlke, C. and Yuan, J. (2003) Pivotal role of oligomerization in expanded polyglutamine neurodegenerative disorders. *Nature*, **421**, 373–379.
31. Kobayashi, Y., Miwa, S., Merry, D.E., Kume, A., Mei, L., Doyu, M. and Sobue, G. (1998) Caspase-3 cleaves the expanded androgen receptor protein of spinal and bulbar muscular atrophy in a polyglutamine repeat length-dependent manner. *Biochem. Biophys. Res. Commun.*, **252**, 145–150.
32. Karpuj, M.V., Becher, M.W., Springer, J.E., Chabas, D., Youssef, S., Pedotti, R., Mitchell, D. and Steinman, L. (2002) Prolonged survival and decreased abnormal movements in transgenic model of Huntington disease, with administration of the transglutaminase inhibitor cystamine. *Nat. Med.*, **8**, 143–149.
33. Panov, A.V., Gutekunst, C.A., Leavitt, B.R., Hayden, M.R., Burke, J.R., Strittmatter, W.J. and Greenamyre, J.T. (2002) Early mitochondrial calcium defects in Huntington's disease are a direct effect of polyglutamines. *Nat. Neurosci.*, **5**, 731–736.
34. La Spada, A.R. and Taylor, J.P. (2003) Polyglutamines placed into context. *Neuron*, **38**, 681–684.
35. Lin, X., Antalffy, B., Kang, D., Orr, H.T. and Zoghbi, H.Y. (2000) Polyglutamine expansion down-regulates specific neuronal genes before pathologic changes in SCA1. *Nat. Neurosci.*, **3**, 157–163.
36. Luthi-Carter, R., Strand, A., Peters, N.L., Solano, S.M., Hollingsworth, Z.R., Menon, A.S., Frey, A.S., Spektor, B.S., Penney, E.B., Schilling, G. *et al.* (2000) Decreased expression of striatal signaling genes in a mouse model of Huntington's disease. *Hum. Mol. Genet.*, **9**, 1259–1271.
37. Wyttenbach, A., Swartz, J., Kita, H., Thykjaer, T., Carmichael, J., Bradley, J., Brown, R., Maxwell, M., Schapira, A., Orntoft, T.F. *et al.* (2001) Polyglutamine expansions cause decreased CRE-mediated transcription and early gene expression changes prior to cell death in an inducible cell model of Huntington's disease. *Hum. Mol. Genet.*, **10**, 1829–1845.
38. Kita, H., Carmichael, J., Swartz, J., Muro, S., Wyttenbach, A., Matsubara, K., Rubinsztein, D.C. and Kato, K. (2002) Modulation of polyglutamine-induced cell death by genes identified by expression profiling. *Hum. Mol. Genet.*, **11**, 2279–2287.
39. Ferrante, R.J., Kubilus, J.K., Lee, J., Ryu, H., Beesen, A., Zucker, B., Smith, K., Kowall, N.W., Ratan, R.R., Luthi-Carter, R. and Hersch, S.M. (2003) Histone deacetylase inhibition by sodium butyrate chemotherapy ameliorates the neurodegenerative phenotype in Huntington's disease mice. *J. Neurosci.*, **23**, 9418–9427.
40. McCampbell, A. and Fischbeck, K.H. (2001) Polyglutamine and CBP: fatal attraction? *Nat. Med.*, **7**, 528–530.
41. Kramer, O.H., Gottlicher, M. and Heinzel, T. (2001) Histone deacetylase as a therapeutic target. *Trends Endocrinol. Metab.*, **12**, 294–300.
42. Kelly, W.K., Richon, V.M., O'Connor, O., Curley, T., MacGregor-Curtelli, B., Tong, W., Klang, M., Schwartz, L., Richardson, S., Rosa, E. *et al.* (2003) Phase I clinical trial of histone deacetylase inhibitor: suberoylanilide hydroxamic acid administered intravenously. *Clin. Cancer Res.*, **9**, 3578–3588.
43. Carducci, M.A., Gilbert, J., Bowling, M.K., Noe, D., Eisenberger, M.A., Sinibaldi, V., Zabelina, Y., Chen, T.L., Grochow, L.B. and Donehower, R.C. (2001) A phase I clinical and pharmacological evaluation of sodium phenylbutyrate on an 120-h infusion schedule. *Clin. Cancer Res.*, **7**, 3047–3055.
44. Egorin, M.J., Yuan, Z.M., Sentz, D.L., Plaisance, K. and Eiseman, J.L. (1999) Plasma pharmacokinetics of butyrate after intravenous administration of sodium butyrate or oral administration of tributyrin or sodium butyrate to mice and rats. *Cancer Chemother. Pharmacol.*, **43**, 445–453.
45. Katsuno, M., Adachi, H., Inukai, A. and Sobue, G. (2003) Transgenic mouse models of spinal and bulbar muscular atrophy (SBMA). *Cytogenet. Genome Res.*, **100**, 243–251.
46. Kobayashi, Y. and Sobue, G. (2001) Protective effect of chaperones on polyglutamine diseases. *Brain Res. Bull.*, **56**, 165–168.
47. Kriz, J., Gowing, G. and Julien, J.P. (2003) Efficient three-drug cocktail for disease induced by mutant superoxide dismutase. *Ann. Neurol.*, **53**, 429–436.
48. Chang, J.G., Hsieh-Li, H.M., Jong, Y.J., Wang, N.M., Tsai, C.H. and Li, H. (2001) Treatment of spinal muscular atrophy by sodium butyrate. *Proc. Natl Acad. Sci. USA*, **98**, 9808–9813.
49. Niwa, H., Yamamura, K. and Miyazaki, J. (1991). Efficient selection for high-expression transfectants with a novel eukaryotic vector. *Gene*, **108**, 193–199.
50. Kobayashi, Y., Kume, A., Li, M., Doyu, M., Hata, M., Ohtsuka, K. and Sobue, G. (2000) Chaperones Hsp70 and Hsp40 suppress aggregate formation and apoptosis in cultured neuronal cells expressing truncated androgen receptor protein with expanded polyglutamine tract. *J. Biol. Chem.*, **275**, 8772–8778.
51. Adachi, H., Kume, A., Li, M., Nakagomi, Y., Niwa, H., Do, J., Sang, C., Kobayashi, Y., Doyu, M. and Sobue, G. (2001) Transgenic mice with an expanded CAG repeat controlled by the human AR promoter show polyglutamine nuclear inclusions and neuronal dysfunction without neuronal cell death. *Hum. Mol. Genet.*, **10**, 1039–1048.
52. Terao, S., Sobue, G., Hashizume, Y., Li, M., Inagaki, T. and Mitsuma, T. (1996). Age-related changes in human spinal ventral horn cells with special reference to the loss of small neurons in the intermediate zone: a quantitative analysis. *Acta Neuropathol.*, **92**, 109–114.

Neuron, Vol. 41, 677–682, March 4, 2004, Copyright ©2004 by Cell Press

Polyglutamine Diminishes VEGF: Passage to Motor Neuron Death?

Altered gene transcription has been implicated in the pathogenesis of polyglutamine-dependent neurodegeneration. In this issue of *Neuron*, Sopher et al. demonstrate that androgen receptors containing expanded polyglutamine cause decreased expression of vascular endothelial growth factor (VEGF) by interfering with cAMP response element binding protein binding protein (CBP), thereby contributing to the motor neuron degeneration in spinal and bulbar muscular atrophy.

Expansion of a triplet nucleotide repeat is the molecular basis for a variety of hereditary neuromuscular diseases. At least nine neurodegenerative diseases result from a tedious trinucleotide CAG repeat, which encodes a polyglutamine tract (reviewed in Zoghbi and Orr, 2000). These disorders, called polyglutamine diseases, include spinal and bulbar muscular atrophy (SBMA), Huntington's disease (HD), spinocerebellar ataxias (SCA1, 2, 3, 6, 7, and 17), and dentatorubral pallidoluysian atrophy (DRPLA). Several shared clinical and histopathological features seen in polyglutamine diseases imply a common pathogenesis. The patients suffer from slow progressive neuromuscular symptoms with the onset in adulthood. Although the causative genes are distinct, selected subsets of neurons in the central nervous system undergo degeneration in each disease. Histopathological hallmarks are the loss of neurons in the affected area and the existence of characteristic intranuclear inclusions in the residual neuronal cells. These inclusions contain aggregates of the causative protein together with fundamental cellular components, providing a clue to the mechanisms causing neurodegeneration. Although the precise role of these inclusions remains open to debate, a large body of evidence suggests that the nuclear localization of aberrant polyglutamine protein is an essential step in the pathogenesis.

The perturbation of gene transcription is likely to be among the most substantial nuclear events in the pathophysiology of polyglutamine diseases. This hypothesis emerged from the observation that cAMP response element binding protein binding protein (CBP), a transcriptional coactivator, is sequestrated into the polyglutamine inclusion (Nucifora et al., 2001). Furthermore, the acetyltransferase activity of CBP is directly inhibited by the interaction with aberrant polyglutamine protein (Steffan et al., 2001). In agreement with these findings, alteration of a wide range of gene expression has been detected in mouse models of polyglutamine diseases (Sugars and Rubinsztein, 2003). It is of therapeutic significance that polyglutamine-mediated neurodegeneration in a *Drosophila* model of HD is alleviated by histone deacetylase inhibitors, which restore histone acetylation and upregulate gene transcriptions (Steffan et al., 2001). Although decreased transcription appears to be a plausible explanation for the pathogenesis, little direct link between CBP dysfunction and neurodegeneration has been clarified in vivo. In addition, it remains unclear which gene is responsible for neuronal cell death in each polyglutamine disease.

Spinal and bulbar muscular atrophy (SBMA), or Kennedy's disease, which is caused by an expanded CAG repeat in the androgen receptor (AR) gene, was the first disease to be identified as a polyglutamine disease (La Spada et al., 1991). SBMA is an adult-onset lower motor neuron disease characterized by proximal muscle atrophy, weakness, fasciculations, and bulbar involvement. In the central nervous system, the brainstem and the anterior horn are selectively involved. Besides motor neuron degeneration, patients present with several systemic complications: gynecomastia, hyperlipidemia, and glucose intolerance. Since the loss of AR function does not result in neuromuscular phenotypes, the extended polyglutamine tract itself appears to render the causative protein toxic, as documented in other polyglutamine diseases. The disruption of CBP-mediated transcription has also been implicated in the pathogenesis of this disease (McCampbell et al., 2001). Despite a common molecular basis, SBMA is distinct from other polyglutamine diseases in that males are exclusively affected. A transgenic mouse model of SBMA revealed that ligand-dependent nuclear translocation of the pathogenic AR protein accounts for the gender-related pathogenesis, leading to the development of a potential hormonal therapy for this disorder (Katsuno et al., 2002). In this issue of *Neuron*, Sopher et al. (2004) report a new transgenic mouse model carrying human AR yeast artificial chromosome (YAC) with a prolonged CAG repeat. Their study reconfirmed the importance of nuclear accumulation of aberrant AR and ligand-dependent pathophysiology in SBMA. Since the expression of the transgene is controlled by its own promoter, the mRNA level of the mutant AR in this model is less than that in previous mouse models using potent exogenous promoters. This would account for the pathological distribution reminiscent of SBMA and the slow progression of motor disability. Among the conspicuous achievements in this study is the finding that the transgenic mice recapitulate the loss of lower motor neurons in SBMA. Whereas histopathological studies of autopsy cases with polyglutamine diseases show a tangible loss of neurons in lesions, a majority of transgenic mouse models demonstrate neuromuscular disability without detectable cell death (Zoghbi and Orr, 2000). This could be explained by the short life span and excessive expression of the causative polyglutamine protein in these mouse models. Symptomatic phenotypes with normal cell populations may indicate that the pathophysiology of polyglutamine disease rises from the dysfunction of neurons. This hypothesis in turn indicates the reversibility of the pathogenesis at the early stage of the diseases. In support of this view, the interruption of mutant gene

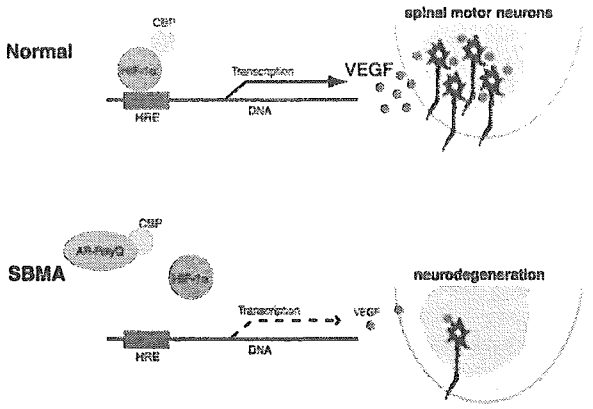

Figure 1. Possible Mechanism of VEGF-Related Motor Neuron Degeneration in SBMA

Hypoxia-inducible factor 1α (HIF-1α) binds to hypoxia-response element (HRE) in the promoter of vascular endothelial growth factor (VEGF), upregulating its transcription. This transactivating activity of HIF-1α is facilitated through interaction with cAMP response element binding protein binding protein (CBP). In spinal and bulbar muscular atrophy (SBMA), the pathogenic androgen receptor (AR) containing expanded polyglutamine (polyQ) interacts with CBP, resulting in decreased level of VEGF. These processes appear to contribute to motor neuron degeneration in SBMA.

expression reversed the symptoms and histopathological features in a conditional mouse model of HD using a tet-regulation system (Yamamoto et al., 2000). Although this observation justifies medical intervention to mildly affected or presymptomatic patients, elucidating the precise mechanism giving rise to neuronal cell death is also essential for the development of therapies for polyglutamine diseases. The study of Sopher et al. appears to offer a striking insight into the pathophysiology of polyglutamine-induced motor neuron death, in their revelation that the interaction between pathogenic AR and CBP results in a reduced expression of vascular endothelial growth factor (VEGF), which appears to contribute to the neurodegeneration in SBMA.

VEGF, first discovered as a factor enhancing vascular permeability, plays a crucial role in physiological and pathological angiogenesis. Diverse biological effects of VEGF are facilitated by its receptor, VEGF-2, also termed kinase insert domain receptor (KDR). The gene expression of VEGF is drastically upregulated upon hypoxia in order to form new blood vessels. Hypoxia-inducible factors, HIF-1α and HIF-2α, mediate this cellular protective response through binding to hypoxia-response element (HRE) in the promoter of VEGF. The transactivating activity of HIF-1α is facilitated through interaction with transcriptional coactivators such as CBP (Figure 1). The depletion of a single allele of VEGF results in embryonic lethality, whereas lack of the HRE sequence in the VEGF promoter leads to slowly progressive motor neuron degeneration (Oosthuyse et al., 2001). Knockin mice harboring a *VEGF* gene in which HRE is deleted demonstrate a late-onset motor neuron disease resembling SBMA and amyotrophic lateral sclerosis (ALS), suggesting a pivotal role for VEGF in neurodegeneration. The low expression level of VEGF in these mice results in loss of spinal motor neurons, axonal degeneration in the peripheral nerve, and neurogenic muscular atrophy, all of which are pathological features of human motor neuron diseases. Moreover, the targeted disruption of HRE results in the marked exacerbation of motor neuron degeneration in transgenic mice carrying mutant superoxide dismutase 1 (SOD 1), the most frequent cause of familial ALS (Lambrechts et al., 2003). The deleterious effects of HRE deletion on motor neurons could be due to the suppression of favorable effects of VEGF: enhancement of blood supply and direct neuroprotection. Given that intraperitoneal administration of VEGF ameliorates ischemia-induced degeneration of spinal motor neurons in the aberrant VEGF knockin mice (Lambrechts et al., 2003), blood circulation insufficiency may cause neuromuscular phenotypes. Since VEGF protects cultured normal motor neurons from apoptotic stimuli, loss of these neurotrophic effects could also contribute to the pathogenesis of motor neuron degeneration due to HRE deletion.

The study of Sopher et al. shows that the reduction in the expression level of VEGF precedes the onset of neurogenic muscular atrophy, suggesting that the transcriptional alteration is a trigger, rather than a consequence, of neurodegeneration. The implication of VEGF in SBMA is also backed by the observation that an exogenous VEGF administration alleviates cytotoxicity induced by pathogenic AR with expanded polyglutamine in their cell model. In addition, CBP cotransfection augments VEGF level in the same cultured motor neurons, implying that the transactivating ability of CBP is suppressed by an aberrant protein-protein interaction with AR. This work sheds light on VEGF as a key player in the pathogenesis of polyglutamine-induced motor neuron degeneration, providing another therapeutic target for SBMA. The retrograde delivery of neurotrophic factors ameliorates neurodegeneration in mouse models of motor neuron diseases to some extent (Kaspar et al., 2003). It should be of value to investigate whether VEGF administration improves the polyglutamine-dependent pathogenesis in the SMBA mouse model of Sopher et al. Alternatively, the repressed transcription of VEGF in SBMA mice suggests that chronic hypoxia aggravates motor neuron degeneration, although its clinical implications have yet to be elucidated. Chronic ischemia, aggravated by lowered level of VEGF, appears to induce oxidative stress, which has been suggested to exacerbate neurodegenerative processes. It thus seems possible that polyglutamine-induced pathophysiology could be ameliorated by antioxidative therapy, which should be tested elsewhere.

A great deal of effort has been made to clarify the exact mechanism causing neuronal dysfunction and the process leading to cell death in polyglutamine diseases. Multiple pathophysiological steps may plunge neurons from dysfunction to death in the presence of an expanded polyglutamine tract. The transcriptional dysregulation of VEGF is likely to play an important role in polyglutamine-induced motor neuron death, since the HRE-deleted mice also showed loss of spinal motor neurons (Oosthuyse et al., 2001). However, whether this hypothesis accounts for the whole pathogenesis of SBMA remains to be resolved. Given that multiple mechanisms are involved in neurodegeneration, we need to clarify which genes, regulated by CBP or other factors,

are responsible for the pathogenesis of polyglutamine diseases. Such clarification would expand therapeutic options for these devastating disorders.

Masahisa Katsuno and Gen Sobue
Department of Neurology
Nagoya University Graduate School of Medicine
Nagoya 466-8550
Japan

Selected Reading

Katsuno, M., Adachi, H., Kume, A., Li, M., Nakagomi, Y., Niwa, H., Sang, C., Kobayashi, Y., Doyu, M., and Sobue, G. (2002). Neuron *35*, 843–854.

Kaspar, B.K., Llado, J., Sherkat, N., Rothstein, J.D., and Gage, F.H. (2003). Science *301*, 839–842.

Lambrechts, D., Storkebaum, E., Morimoto, M., Del-Favero, J., Desmet, F., Marklund, S.L., Wyns, S., Thijs, V., Andersson, J., van Marion, I., et al. (2003). Nat. Genet. *34*, 383–394.

La Spada, A.R., Wilson, E.M., Lubahn, D.B., Harding, A.E., and Fischbeck, K.H. (1991). Nature *352*, 77–79.

McCampbell, A., Taye, A.A., Whitty, L., Penney, E., Steffan, J.S., and Fischbeck, K.H. (2001). Proc. Natl. Acad. Sci. USA *98*, 15179–15184.

Nucifora, F.C., Jr., Sasaki, M., Peters, M.F., Huang, H., Cooper, J.K., Yamada, M., Takahashi, H., Tsuji, S., Troncoso, J., Dawson, V.L., et al. (2001). Science *291*, 2423–2428.

Oosthuyse, B., Moons, L., Storkebaum, E., Beck, H., Nuyens, D., Brusselmans, K., Van Dorpe, J., Hellings, P., Gorselink, M., Heymans, S., et al. (2001). Nat. Genet. *28*, 131–138.

Sopher, B.L., Thomas, P.S., Jr., LaFevre-Bernt, M.A., Holm, I.E., Wilke, S.A., Ware, C.B., Jin, L.-W., Libby, R.T., Ellerby, L.M., and La Spada, A.R. (2004). Neuron *41*, this issue, 687–699.

Steffan, J.S., Bodai, L., Pallos, J., Poelman, M., McCampbell, A., Apostol, B.L., Kazantsev, A., Schmidt, E., Zhu, Y.Z., Greenwald, M., et al. (2001). Nature *413*, 739–743.

Sugars, K.L., and Rubinsztein, D.C. (2003). Trends Genet. *19*, 233–238.

Yamamoto, A., Lucas, J.J., and Hen, R. (2000). Cell *101*, 57–66.

Zoghbi, H.Y., and Orr, H.T. (2000). Annu. Rev. Neurosci. *23*, 217–247.

Field strengths and sequences influence putaminal MRI findings in multiple system atrophy

H. Watanabe, MD; H. Fukatsu, MD; N. Hishikawa, MD; Y. Hashizume, MD; and G. Sobue, MD

Multiple system atrophy (MSA) is a sporadic neurodegenerative disease that is difficult to diagnose. MRI can show signal abnormalities such as putaminal hyperintensity, hyperintense putaminal rim, and significant putaminal hypointensity, strengthening a diagnosis of MSA.[1-7] However, these abnormalities are highly variable among the published cases and reports.[1-7] Differences of magnetic field strengths and sequences and pathologic features could explain such variability of putaminal signal changes, but the precise nature of putaminal signal changes remains unclear.[1-7]

We report an MRI study of the cadaveric tissue from a patient with MSA performed to investigate putaminal signal changes with different magnetic field strengths and then correlated the findings with histopathologic observations.

Case report. A 54-year-old man first noticed gait disturbance at age 48 years and dysuria and erectile dysfunction at age 49 years, all of which steadily worsened. Neurologic examinations at age 50 years revealed urinary dysfunction and parkinsonism poorly responsive to L-dopa, including bradykinesia, rigidity, and postural instability. His condition worsened progressively, and he died of pneumonia 6 years after onset of illness.

Autopsy was performed 3 hours post-mortem. The brain was fixed in 10% buffered formalin. A 2-cm coronal section that included the putamen was used for MRI examination with 0.35-T (OPART, Japan) and 1.5-T (VISART, Japan) scanners using a surface coil. Images were obtained in the coronal plane using T2-weighted fast spin-echo (FSE) at 0.35 T and 1.5 T (2,000/120/5) and T2*-weighted gradient echo (GE) sequences (38/24/5; flip angle, 15) at 1.5 T. For all sequences, a 3-mm slice thickness, a field of view of 75 × 75 mm, and a matrix of 192 × 192 mm were used.

T2-weighted FSE at 0.35 T showed marked putaminal hyperintensity, whereas T2-weighted FSE at 1.5 T showed little signal change in the putamen except for mild hyperintensity in the outer margin. T2*-weighted GE at 1.5 T, representing the most sensitive MRI sequences for evaluation of putaminal iron deposition, showed low intensity (figure, A through C). For histopathologic evaluation, 5-μm-thick paraffin-embedded sections were prepared from the same position and stained with hematoxylin and eosin, Holzer, Gallyas–Braak, Bodian, and Prussian blue stains. Neuronal loss and gliosis were noted, as were glial cytoplasmic inclusions, all typical histopathologic findings for MSA. The Holzer stain showed severe gliosis predominantly in the dorsolateral putamen (figure, D). No calcification was present. Extracellular and intracellular iron deposits were present extensively in this area (figure, E). The high signal intensity on T2-weighted FSE at 0.35 T was highly consistent with the distribution of gliosis. Conversely, the low intensity on T2*-weighted GE at 1.5 T corresponded well to the region of iron deposits.

Discussion. This is the first study to correlate putaminal MRI findings at different magnetic field strengths and sequences in postmortem MSA brain with histologic findings. Although artifact from formalin and varying relaxation rates caused by a different hydration state of the tissue should be considered, direct comparison of post-mortem MRI and histologic findings would be beneficial particularly for understanding MR signal differences in the putamen of patients with MSA because putaminal findings at autopsy could differ from those at examination of MRI during life.

MRI using FSE at 1.5 T, which is used widely for diagnosis of MSA, showed only mild hyperintensity in the outer putaminal margin, which can be observed even in healthy subjects. Conversely, FSE at 0.35 T and GE at 1.5 T revealed significant putaminal hyperintensity and hypointensity. Histopathologic study showed severe gliosis and an increase in ferritin deposition, particularly in the dorsolateral putamen. Gliosis probably increased signal intensity in T2-weighted images, whereas ferritin enhanced T2 relaxation in the order FSE at 0.35 T, FSE at 1.5 T, and GE at 1.5 T. Taken together, topography of gliosis predominantly in dorsolateral parts, severities of gliosis and iron deposits, and magnetic field strengths and sequences would determine the putaminal MRI findings and can result in a normal putaminal appearance under FSE at 1.5 T despite the presence of pathologic change. In contrast, the higher insensitivity to paramagnetic effects can provide the hyperintensity at 0.35 T.

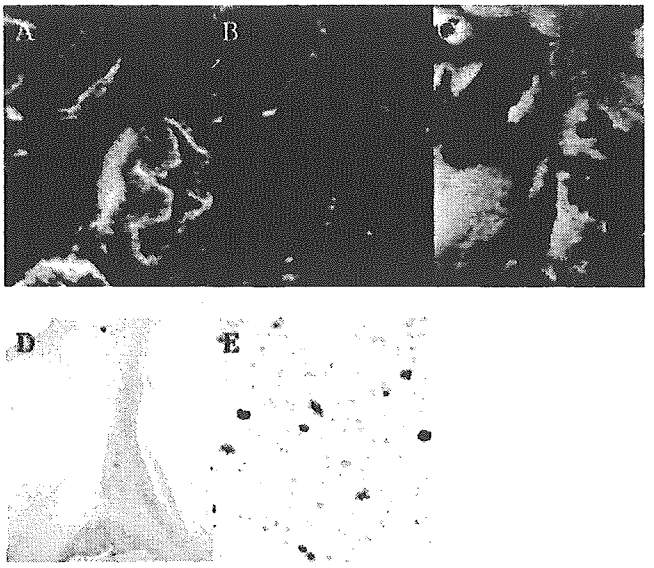

Figure. (A) MRI operated at T2-weighted fast spin-echo (FSE) at 0.35 T. Significant putaminal hyperintensity is evident. (B) MRI operated at T2-weighted FSE at 1.5 T. The greater part of the putamen shows isointensity except for mild hyperintensity of the rim at the outer margin. (C) MRI operated at T2-weighted gradient echo at 1.5 T. Severe putaminal hypointensity is observed. (D) Holzer stain. Exclusive severe gliosis is seen in the putamen. (E) Prussian blue stain. An increase in ferritin deposits is widespread in the putamen. Original magnification, ×400.*

Putaminal hyperintensity in MRI was first described as a finding typical to MSA.[1] Many subsequent reports have confirmed this, but sensitivity and specificity were found to be highly variable.[2-7] In MR survey of patients with MSA, it should be considered that histopathologic features differentially affect MR findings at different magnetic field strengths and sequences.

From the Departments of Neurology (Drs. Watanabe, Hishikawa, and Sobue) and Radiology (Dr. Fukatsu), Nagoya University Graduate School of Medicine, Japan; and Institute for Medical Science of Aging (Dr. Hashizume), Aichi Medical University, Japan.

Received May 30, 2003. Accepted in final form October 17, 2003.

Address correspondence and reprint requests to Dr. Gen Sobue, Department of Neurology, Nagoya University Graduate School of Medicine, Nagoya 466-8550 Japan; e-mail: sobueg@med.nagoya-u.ac.jp

References

1. Savoiardo M, Strada L, Girotti F, et al. MR imaging in progressive supranuclear palsy and Shy-Drager syndrome. J Comput Assist Tomogr 1989;13:555–560.
2. Schwarz J, Weis S, Kraft E, et al. Signal changes on MRI and increases in reactive microgliosis, astrogliosis, and iron in the putamen of two patients with multiple system atrophy. J Neurol Neurosurg Psychiatry 1996;60:98–101.
3. Schrag A, Kingsley D, Phatouros C, et al. Clinical usefulness of magnetic resonance imaging in multiple system atrophy. J Neurol Neurosurg Psychiatry 1998;65:65–71.
4. Kraft E, Schwarz J, Trenkwalder C, Vogl T, Pfluger T, Oertel WH. The combination of hypointense and hyperintense signal changes on T2-weighted magnetic resonance imaging sequences: a specific marker of multiple system atrophy? Arch Neurol 1999;56:225–228.
5. Watanabe H, Saito Y, Terao S, et al. Progression and prognosis in multiple system atrophy: an analysis of 230 Japanese patients. Brain 2002; 125:1070–1083.
6. Kraft E, Trenkwalder C, Auer DP. T2*-weighted MRI differentiates multiple system atrophy from Parkinson's disease. Neurology 2002;59:1265–1267.
7. Bhattacharya K, Saadia D, Eisenkraft B, et al. Brain magnetic resonance imaging in multiple-system atrophy and Parkinson's disease: a diagnostic algorithm. Arch Neurol 2002;59:835–842.

Sweet relief for Huntington disease

Masahisa Katsuno, Hiroaki Adachi & Gen Sobue

Oral delivery of a simple, nontoxic sugar molecule alleviates symptoms of Huntington disease in a mouse model (pages 148–154).

A CAG repeat was first pinned to a neurological disorder—spinal and bulbar muscular atrophy (SBMA)—in 1991 (ref. 1). The pathological influence of the affected gene, an androgen receptor, eventually paled beside the growing realization that the repeat itself was key to the disease. A number of other neurological diseases have since been linked to glutamine-encoding CAG repeats, most prominent among them Huntington disease.

Despite the excitement they have sparked, these discoveries have as yet done little to improve the lives of patients, including more than 35,000 with Huntington disease in the United States. In this issue, Tanaka *et al.* move us closer to reaping the benefits of this decade of research. The authors report that in mouse models of Huntington disease, treatment with a nontoxic sugar substance can prevent the development of the brain pathology associated with Huntington disease, and can delay the progress of symptoms such as motor dysfunction. The approach stands out as the most exciting therapeutic prospect to date for Huntington disease, and also holds promise for the entire class of polyglutamine disorders.

In addition to Huntington disease and SBMA, other polyglutamine disorders include several forms of spinocerebellar ataxia, as well as dentatorubral pallidoluysian atrophy[2]. Outside of the polyglutamine stretch, each causative protein seems unrelated, and removal of the causative protein genetically or by other means does not result in disease in humans or animal models[2]. Yet the diseases show phenotypic similarities. The clinical features depend at least partially on the number of CAG repeats, and are influenced by the meiotic instability of the repeat length. These clinical and genetic similarities imply that polyglutamines induce toxicity, although loss of the normal function of causative proteins may influence the disease[3].

Masahisa Katsuno, Hiroaki Adachi and Gen Sobue are in the Department of Neurology, Nagoya University Graduate School of Medicine, Nagoya, 65 Tsurumai-cho, Showa-ku, Nagoya 466-8550, Japan.
e-mail: sobueg@med.nagoya-u.ac.jp

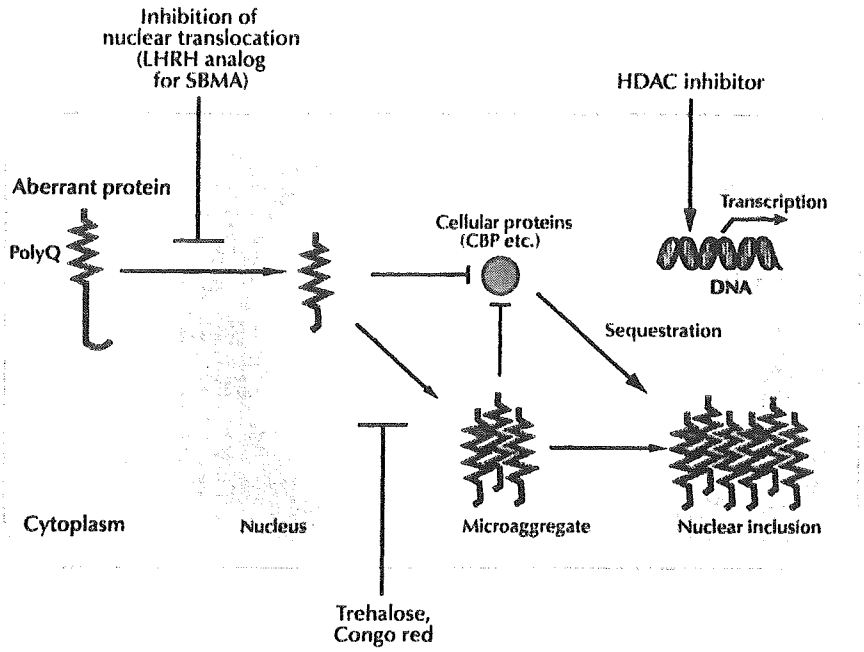

Figure 1 Therapeutic approaches for polyglutamine diseases. Several approaches attempt to mitigate the toxicity of polyglutamine (poly Q) tract–containing proteins. Leuprorelin prevents nuclear uptake of mutant androgen receptor, resulting in the rescue of neuromuscular phenotypes of SBMA. Histone deacetylase inhibitors ameliorate transcription of affected cells. Tanaka *et al.* found that a disaccharide, trehalose, inhibits aggregation of a protein with an expanded polyglutamine tract, especially in the nucleus (as does Congo red). LHRH, luteinizing hormone–releasing hormone; CBP, CREB-binding protein.

How do the glutamine repeats affect the cell? The expansion of the polyglutamine tract alters protein conformation, resulting in the formation of insoluble aggregates. These aggregates sequester normal cellular proteins such as transcription factors, heat shock proteins, ubiquitin, and proteasome components. The propensity of the polyglutamine-containing proteins to aggregate depends on the length of the polyglutamine stretch and is enhanced by protein cleavage through caspase activation.

Patients with polyglutamine diseases show loss of specific types of neurons. The cells that do not die contain inclusions rich in polyglutamine-containing proteins, mainly in the nucleus. These inclusions are found in the vulnerable neurons, implying a direct role in pathogenesis. Whether these aggregates are toxic—a notion supported by a large body of evidence—or reflect a protective response is controversial.

A dramatic study earlier this year bolstered arguments in favor of toxicity. Injection of the dye Congo red prevented formation of nuclear inclusions and alleviated symptoms in a mouse model of Huntington disease[4].

Tanaka *et al.*, favoring the notion that the aggregates are toxic, sought a new aggregation inhibitory therapy for Huntington disease[5]. The authors first used an *in vitro* aggregate formation assay, with myoglobin containing an expanded polyglutamine tract as a target molecule. Using this screening system, they discovered that disaccharides potently inhibited aggregate formation. Trehalose, the most effective disaccharide, selectively stabilized a protein containing a long polyglutamine tract, but not a protein with the normal number of glutamines. The authors confirmed this stabi-

lization in a cell model expressing the aberrant form of huntingtin, the causative protein of Huntington disease. The stabilization of myoglobin with an elongated polyglutamine tract results[6] accounts for the trehalose-mediated suppression of aggregation formation.

The authors went on to test transgenic mouse models of Huntington disease. They found that trehalose-treated mice had fewer nuclear inclusions than untreated mice. Trehalose also improved motor dysfunction and prolonged survival, without any deleterious side effects. The extremely low toxicity and high water-solubility of this compound make this an attractive therapeutic approach, although the therapeutic effects seem to result from prevention of new aggregate formation, not from reversal of the pathology. The data reinforce the rationale of aggregation-inhibitory therapy for polyglutamine diseases (Fig. 1). Trehalose is now ready for phase 1 safety trials in humans.

Other approaches to polyglutamine disease also show promise. Nuclear accumulation of polyglutamine-containing proteins before aggregate formation is probably an essential step in pathogenesis. A mutation that inactivates the nuclear localization signal in ataxin-1, the causative protein in spinocerebellar ataxia-1, nullifies polyglutamine-induced neurodegeneration in a transgenic mouse model[7]. In cell culture, chemically synthesized polyglutamine peptides induce neuronal cell death only when they are directed into the nucleus[8]. These observations suggest that nuclear-directed transport of mutant proteins is an alternative target of intervention (Fig. 1), although cytosolic events should not be neglected[3].

Androgen deprivation therapy in a transgenic mouse model of SBMA clearly demonstrates the usefulness of this therapeutic strategy[9]. A luteinizing hormone–releasing hormone analog, leuprorelin, prevents nuclear translocation of polyglutamine-containing androgen receptor protein, resulting in a significant improvement of disease[9]. A clinical trial with leuprorelin, currently under way in Japan, should clarify the clinical benefit of this drug for SBMA patients.

Transcriptional dysregulation, an event downstream of polyglutamine aggregation, can also be targeted (Fig. 1). Transcriptional coactivators including CREB-binding protein are sequestrated in the inclusion, and are also enfeebled by interaction with soluble polyglutamine tract–containing proteins[3]. An increase in acetylation of nuclear histone proteins, facilitated by histone deacetylase inhibitors, ameliorates neurodegeneration in a mouse model of Huntington disease[10,11]. These compounds have also been used for patients with malignancies. Clinical trials of histone deacetylase inhibitors should be planned carefully, however, taking the hazardous side effects into account.

The promising results of these preclinical studies are ushering in a new era in polyglutamine research: the therapeutic stage. The new investigations also encourage us to continue to search for new, clinically applicable compounds such as aggregation inhibitors. The intensive basic research is bearing fruit, and shows promise of continuing to do so as we move into clinical trials.

1. La Spada, A.R. *et al. Nature* **352**, 77–79 (1991).
2. Zoghbi, H.Y. & Orr, H.T. *Annu. Rev. Neurosci.* **23**, 217–247 (2000).
3. Ross, C.A. *Neuron* **35**, 819–822 (2002).
4. Sanchez, I. *et al. Nature* **421**, 373–379 (2003)
5. Tanaka, M. *et al. Nat. Med.* **10**, 148–154 (2004).
6. Tanaka, M. *et al. J. Biol. Chem.* **276**, 45470–45475 (2001)
7. Klement, I.A. *et al. Cell* **95**, 41–53 (1998).
8. Yang, W. *et al. Hum. Mol. Genet.* **11**, 2905–2911 (2003).
9. Katsuno, M. *et al. Nat. Med.* **9**, 768–773 (2003).
10. Hockly, E. *et al. Proc. Natl. Acad. Sci. USA* **100**, 2041–2046 (2003).
11. Ferrante, R.J. *et al. J. Neurosci.* **23**, 9418–9427 (2003).

PAPER

Multiple regional ^{1}H-MR spectroscopy in multiple system atrophy: NAA/Cr reduction in pontine base as a valuable diagnostic marker

H Watanabe, H Fukatsu, M Katsuno, M Sugiura, K Hamada, Y Okada, M Hirayama, T Ishigaki, G Sobue

J Neurol Neurosurg Psychiatry 2004;**75**:103–109

See end of article for authors' affiliations

Correspondence to: Gen Sobue, MD, Department of Neurology, Nagoya University Graduate School of Medicine, Nagoya 466-8550 Japan; sobueg@med.nagoya-u.ac.jp

Received 20 December 2002
In revised form 31 March 2003
Accepted 17 May 2003

Objective: We performed ^{1}H-MR spectroscopy (^{1}H-MRS) on multiple brain regions to determine the metabolite pattern and diagnostic utility of ^{1}H-MRS in multiple system atrophy (MSA).
Methods: Examining single voxels at 3.0 T, we studied metabolic findings of the putamen, pontine base, and cerebral white matter in 24 MSA patients (predominant cerebellar ataxia (MSA-C), n = 13), parkinsonism (MSA-P), n = 11), in 11 age and duration matched Parkinson's disease patients (PD) and in 18 age matched control subjects.
Results: The *N*-acetylaspartate to creatine ratio (NAA/Cr) in MSA patients showed a significant reduction in the pontine base ($p<0.0001$) and putamen ($p = 0.02$) compared with controls. NAA/Cr in cerebral white matter also tended to decline in long standing cases. NAA/Cr reduction in the pontine base was prominent in both MSA-P ($p<0.0001$) and MSA-C ($p<0.0001$), and putaminal NAA/Cr reduction was significant in MSA-P ($p = 0.009$). It was also significant in patients who were in an early phase of their disease, and in those who showed no ataxic symptoms or parkinsonism, or did not show any MRI abnormality of the "hot cross bun" sign or hyperintense putaminal rims. NAA/Cr in MSA-P patients was significantly reduced in the pontine base ($p = 0.001$) and putamen ($p = 0.002$) compared with PD patients. The combined ^{1}H-MRS in the putamen and pontine base served to distinguish patients with MSA-P from PD more clearly.
Conclusions: ^{1}H-MRS showed widespread neuronal and axonal involvement in MSA. The NAA/Cr reduction in the pontine base proved highly informative in the early diagnosis of MSA prior to MRI changes and even before any clinical manifestation of symptoms.

Multiple system atrophy (MSA) is a sporadically occurring neurodegenerative disease that presents parkinsonism, cerebellar ataxia, autonomic failure, and pyramidal signs of varying severity during the course of illness.[1–3] Neuropathological findings consist of a varying neuronal loss, gliosis, and demyelination with widespread regional involvement, particularly including the striatonigral, olivopontocerebellar, and autonomic nervous systems.[4–6] The tempo and progression of multiple system involvement vary widely among individual MSA patients and have been closely related to both functional deterioration and prognosis by clinical evaluation.[7] Thus, assessing the multi-regional involvement in MSA is essential for accurate diagnosis, counselling of patients and families, optimal management of symptoms, and the usefulness of future therapeutic trials.

Proton magnetic resonance spectroscopy (^{1}H-MRS) is a valuable non-invasive MR technique for monitoring brain metabolism in vivo.[8–18] The major peaks of the ^{1}H-MRS spectrum, corresponding to *N*-acetylaspartate (NAA), creatine (Cr), and choline (Cho) containing phospholipids, have been used to evaluate neuronal loss and active myelin breakdown. The ratio of NAA to Cr (NAA/Cr) is considered a metabolic marker reflecting the functional status of neurones and axons in the brain, with a decrease indicating neuronal or axonal loss or dysfunction. Previous studies using ^{1}H-MRS in MSA with predominant parkinsonism (MSA-P) reported a significant NAA/Cr reduction in the striatum compared with Parkinson's disease (PD) patients and normal subjects.[11–14] However, the pontine base and cerebral white matter, which are also pathologically involved in MSA, have not been fully assessed by ^{1}H-MRS. Recent technical innovations have permitted ^{1}H-MRS at higher magnetic field strengths.[19–21] Multi-regional data can be obtained from single voxel ^{1}H-MRS within a short examination time with increasing signal to noise ratio (SNR).

Our purpose was to assess the extent of multiple system involvement in patients with MSA by using multiple regional single voxel ^{1}H-MRS including the putamen, pontine base, and cerebral white matter (CWM), and to further assess the diagnostic value of the regional ^{1}H-MRS.

METHODS

All patients and control subjects gave written informed consent. The MR protocol was approved by the Ethics Committee of the Nagoya University School of Medicine. Twenty four patients with MSA (12M, 12F; mean (SD) age 61 (7) years old), 11 patients with PD (5M, 6F; 63 (9) years old), and 18 control subjects with no history of any neurological disease (10M, 8F; 59 (7) years old) were studied. No significant differences in male to female ratio or age were noted among the three groups. The duration from initial

Abbreviations: Cho, choline; Cr, creatine; CWM, cerebral white matter; HCB, "hot cross bun"; HPR, hyperintense rim; MRI, magnetic resonance imaging; MRS, magnetic resonance spectroscopy; MSA, multiple system atrophy; MSA-C, multiple system atrophy with cerebellar ataxia predominant; MSA-P, multiple system atrophy with parkinsonism predominant; NAA, *N*-acetylaspartate; PD, Parkinson's disease; SNR, signal to noise ratio; VOI, volume of interest.

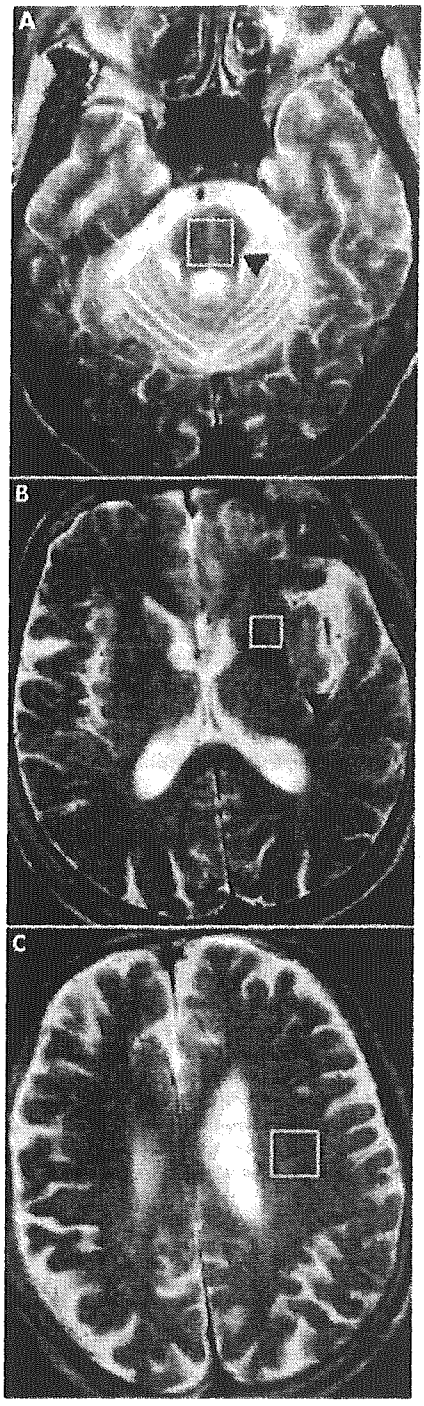

Figure 1 Location of volumes of interest are shown by squares in the pontine base (A), putamen (B), and white matter of the frontal lobe (C). Additionally, in these images, an HCB sign is present in the pons (A), as is a hyperintense putaminal rim (B). Axial T2 weighted images (3.0 T; TR: 3970, TE: 80), with respective findings are indicated by arrowheads.

symptoms to MRI and MRS evaluation also showed no differences between MSA and PD patients (MSA; 3.7 (2.4) years; PD; 4.4 (2.2) years, $p>0.4$). Diagnoses of all MSA and PD patients were "probable" according to established diagnostic criteria.[3 23] As for subtypes of MSA, cerebellar dysfunction (MSA-C) predominated in 13 patients and parkinsonism (MSA-P) in 11. We classified patients into two groups according to the presence of parkinsonian signs in MSA, based on the consensus statement for MSA diagnosis. Patients with bradykinesia plus at least one sign of either rigidity, postural instability, or tremor were considered to manifest parkinsonism and designated as "parkinsonism+", while others were taken to be "parkinsonism−". As for cerebellar dysfunction, patients with gait ataxia plus at least one sign of ataxic dysarthria, limb ataxia, or sustained gaze evoked nystagmus were considered "ataxia+", and others as "ataxia−" based on the consensus criteria.[3] Six of nine MSA-P patients and all PD patients were taking medication for parkinsonism (benserazide/levodopa 25/100 mg, or carbidopa/levodopa 10/100 mg, two or three times daily). All PD patients showed a good response to treatment.

MRI and ^{1}H-MRS were performed with a 3.0 T system (Bruker, Ettlingen, Germany) using a standard head coil with circular polarisation. The imaging protocol consisted of sagittal T1 weighted spin echo sequences (repetition time (TR), 460 ms; echo time (TE), 14 ms) and transverse T2 weighted sequences (TR, 3970 ms; TE, 80 ms). Slice thickness was 6 mm with a 1.2 mm gap and a 512×384 matrix. We evaluated whether a "hot cross bun" (HCB) sign was present in the pons and whether the putamen showed a hyperintense rim (HPR), according to the criteria described in previous reports (fig 1A, B).[7 25–26] The spectroscopic volume of interest (VOI) was placed in the pontine base (2.2 to 3.4 cm^3), the putamen (1 cm^3), and the CWM (3.4 cm^3; fig 1A to C). Voxel size was chosen to be as small as possible while maintaining an acceptable SNR in order to minimise the partial volume effect. Care was taken not to incorporate cerebrospinal fluid spaces within a VOI. The VOI in the putamen was placed on the more affected side, and the frontal lobe VOI was ipsilateral to the putaminal VOI. ^{1}H-MR spectra were acquired using a point resolved spectroscopy sequence with chemical shift selective water suppression. Spectral parameters were as follows: TR: 2000 ms; TE: 30 ms; averages: 256 in the putamen, and 64 each in the centrum semiovale and pons; data points: 1024. A shimming procedure focused on the water signal was performed to obtain a uniform and homogenous magnetic field. After Fourier transformation and zero order phase correction, relative metabolite concentrations for NAA at 2.0 ppm, Cr at 3.0 ppm, and Cho at 3.2 ppm were determined by Lorentzian curve fitting of the corresponding resonance in the frequency spectra. The baseline was corrected for purposes of data presentation. From these data, the metabolite ratios NAA/Cr, and Cho/Cr were determined as semiquantitative values. Post-procedural processing was performed by the same radiologist (HF). All preconditioning, spectroscopic measurements, and processing were performed with Paravision 2.01 software (Bruker). Total examination time including MRI and ^{1}H-MRS was <1 hour. One MSA-C patient with severe pontine atrophy was excluded because a good pontine spectrum could not be obtained.

Values obtained were entered into a database for further statistical analysis. The Mann-Whitney U test and the Kruskal-Wallis test for nonparametric statistics were performed as appropriate. When the Kruskal-Wallis test indicated differences among groups, in a multiple comparison analysis, Scheffé's test was used to identify which group differences accounted for the significant p value. Relationships of NAA/Cr reduction to duration of illness were analysed using Pearson's correlation coefficient. Calculations were performed using the Stat View statistical software package (Abacus Concepts, Berkeley, CA, USA). Statistical significance was defined as $p<0.05$.

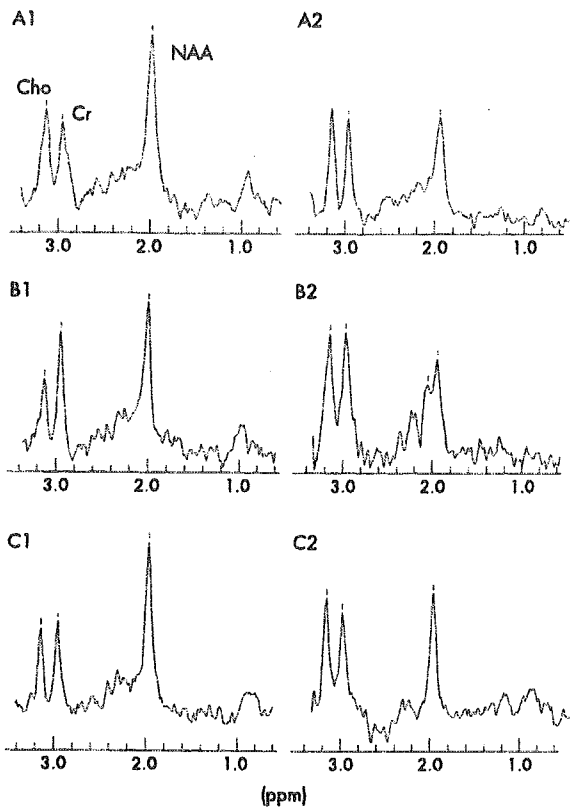

Figure 2 Representative ^{1}H-MRS spectra from control and MSA subjects. A1, B1, and C1 represent spectra from a control subject's pontine base, putamen, and cerebral white matter, respectively. A2, B2, and C2 represent spectra from those same three regions in an MSA patient. NAA, *N*-acetylaspartate; Cho, choline; Cr, creatine; MSA, multiple system atrophy; CWM, cerebral white matter.

RESULTS

Widespread NAA/Cr reduction in MSA in multiple regional ^{1}H-MRS

A representative MSA patient (fig 2) showed a marked reduction of the NAA peak in the pontine base, putamen, and cerebral white matter compared with controls. NAA/Cr was significantly reduced in the pontine base of MSA patients ($p<0.0001$) and in the putamen ($p = 0.02$) compared with controls. MSA patients also showed a lower NAA/Cr in cerebral white matter than controls, but this difference was not statistically significant ($p = 0.12$). Cho/Cr was only slightly increased in MSA, and no significant differences were found among the three groups for the pontine base, putamen, and CWM.

Prominent NAA/Cr reduction in pontine base in both MSA-C and MSA-P

Significant reductions of NAA/Cr were evident in the pontine base, putamen, and CWM in MSA-C and MSA-P compared with controls (fig 3A–C). MSA-C patients showed a significant reduction of NAA/Cr in the pontine base ($p<0.0001$) and CWM ($p = 0.02$), but not in the putamen. MSA-P patients showed a significant reduction of NAA/Cr in the pontine base ($p<0.0001$) and putamen ($p = 0.009$) but not in the CWM. These observations indicate that the NAA/Cr reduction in the pontine base was significant in both MSA-C and MSA-P. Cho/Cr was not changed in MSA-P or MSA-C compared with controls.

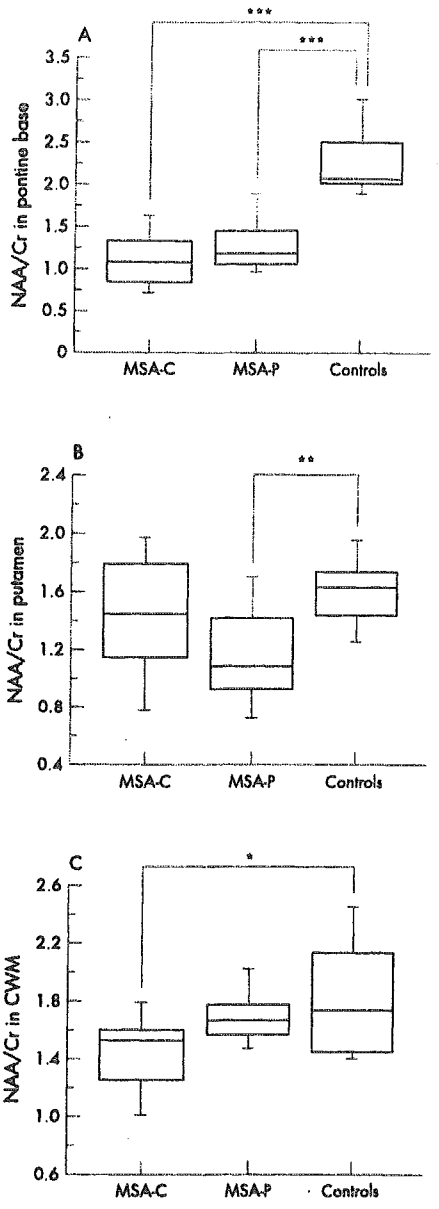

Figure 3 Box and whisker plot of the NAA/Cr ratio. Horizontal lines indicate median values. Boxes extend from the 25th to the 75th percentile. A, B, and C respectively show NAA/Cr in the pontine base, putamen, and cerebral white matter, comparing MSA-C, MSA-P, and control subjects. *$p = 0.02$, **$p = 0.009$, and ***$p<0.0001$ by Scheffé's test, respectively. NAA, *N*-acetylaspartate; Cr, creatine; Cho, choline containing component; MSA-C, multiple system atrophy with cerebellar ataxia predominant; MSA-P, multiple system atrophy with parkinsonism predominant.

Relation of NAA/Cr reduction in pontine base with disease phase, motor symptoms and MRI abnormalities in MSA

In terms of disease duration, the NAA/Cr reduction was most significant in the pontine base of patients with MSA even in an early phase of illness (fig 4). A tendency toward an inverse

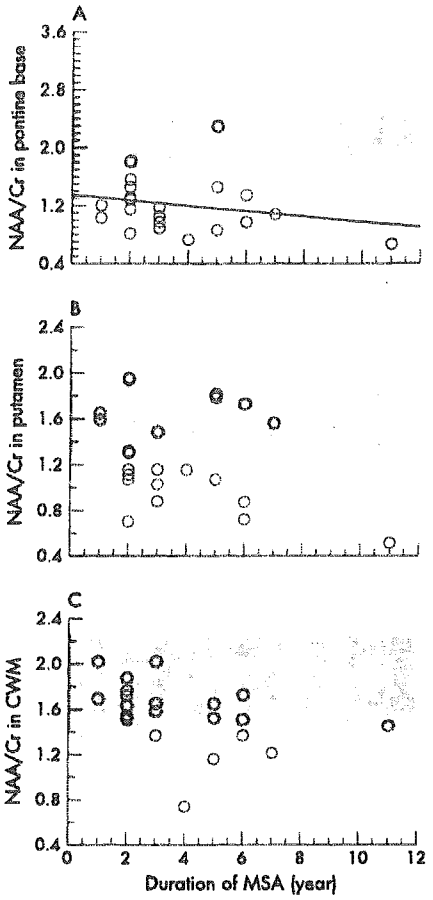

Figure 4 Correlation with duration of MSA of individual NAA/Cr ratios in the pontine base (A), putamen (B), and cerebral white matter (C). The shaded area corresponds to the mean (SD) of NAA/Cr in control subjects. NAA, N-acetylaspartate; Cr, creatine; CWM, cerebral white matter; MSA, multiple system atrophy.

relationship between disease duration and NAA/Cr in the three regions was observed, but did not attain significance (pontine base: $r = -0.24$, $p = 0.29$; putamen: $r = -0.32$, $p = 0.14$; CWM: $r = -0.41$, $p = 0.06$). NAA/Cr in the pontine base was significantly reduced compared with controls even in patients who did not show ataxic symptoms ($p = 0.0006$, fig 5A-1). However, NAA/Cr in the putamen and white matter was not reduced in patients with ataxia (fig 5B-1, C-1). NAA/Cr in the putamen was markedly decreased in MSA patients with parkinsonism ($p = 0.02$, Fig 5B-2), whereas patients without it exhibited no significant reduction compared with controls. NAA/Cr reduction in the pontine base, on the other hand, was significant ($p<0.0001$) irrespective of parkinsonism (Fig 5A-2).

The MRI revealed the HCB sign in the pontine base in eleven MSA patients (46%) and the HPR sign in six (25%). A significant reduction of NAA/Cr was seen in the pontine base even in patients without ($p<0.0001$) as well as in those with an HCB sign ($p<0.0001$; fig 5A-3). In the putamen and cerebral white matter, NAA/Cr values did not show any significant difference irrespective of the HCB sign (fig 5B-3, C-3). Moreover, NAA/Cr significantly decreased in the pontine base in patients both with and without HPR (fig 5A-4). NAA/Cr in the putamen and cerebral white matter did not show any significant differences irrespective of HPR signs (fig 5B-4, C-4). Cho/Cr had no significant relationship to ataxic, parkinsonism, or MRI abnormalities.

NAA/Cr in pontine base in MSA-P and PD

NAA/Cr reduction in the pontine base was highly significant in patients with MSA-P compared with both controls and PD ($p<0.0001$, $p = 0.001$; fig 6A). NAA/Cr in the putamen in MSA-P patients also showed a significant decrease compared with both controls and PD ($p = 0.003$, $p = 0.002$; fig 6B). No significant differences in NAA/Cr were noted in cerebral white matter between MSA-P and PD. These data indicate that the NAA/Cr reduction in the pontine base is a valuable marker to discriminate MSA-P from PD. In addition, combining individual NAA/Cr values for the pontine base and putamen further reduced the overlap between MSA-P and PD (fig 6D), suggesting that a combined assessment of the pontine base and putamen was more effective in discriminating between MSA-P and PD than individual area assessments. Cho/Cr did not display any significant changes in the pontine base, putamen or cerebral white matter.

DISCUSSION

We demonstrated widespread NAA/Cr reduction in the pontine base, putamen and in some cases, in the cerebral hemisphere, but no significant Cho/Cr alteration in patients with MSA using localised ^{1}H-MRS at 3.0 T. In this study, absolute metabolite concentrations were not measured. However, the specific conditions that may change the total Cr signal, such as trauma, hyperosmolar conditions, hypoxia, stroke, and tumours, were not included. Age was matched among MSA, PD, and control groups. Moreover, quantitative studies did not show significant Cr changes between MSA patients and control subjects.[11 16] Thus, the reduction of the NAA/Cr ratio in the present study can be considered due to a selective decrease in NAA levels.

NAA has been immunohistochemically demonstrated to localise almost exclusively within neurones and axons,[27 28] but some in vitro studies have also detected NAA expression in mature, immature, and undifferentiated oligodendrocytes.[29 30] Nevertheless, according to a recent study, in vivo MRS measurements of NAA remain axon specific, with no oligodendrocytes, nonproliferating oligodendrocyte progenitor cells, or myelin contributing to detectable NAA in the mature CNS.[31] This result supports the view that the widespread NAA/Cr reductions observed in this study ultimately reflect widespread neuronal and axonal involvement in MSA, although oligodendrocytes might influence the NAA levels to some degree.

The striking observation in this study is that the NAA/Cr reduction in the pontine base was the most significant among the three regions examined. That reduction was detected in the early phase of illness even in patients with no symptoms of ataxia or parkinsonism, or in patients without MRI abnormality of the HCB sign. Moreover, the pontine NAA/Cr reduction was significant even in MSA-P patients. In addition, NAA/Cr reductions in the pontine base were seen even in patients with no HPR sign in the lateral putamen. These observations suggest that NAA/Cr reduction in the pontine base is an accurate diagnostic marker for MSA even in patients in an early stage and a pre-symptomatic phase of ataxia or parkinsonism. The diagnostic focus of ^{1}H-MRS in MSA has been on the putamen,[11-14] whereas our results unequivocally demonstrated that MRS abnormality can be detected sooner and more universally in the pontine base than in the putamen in the course of the disease. The question is why a significant NAA/Cr reduction can be detected more readily in the pontine base than in the putamen. One reason may be that neuroaxonal degeneration

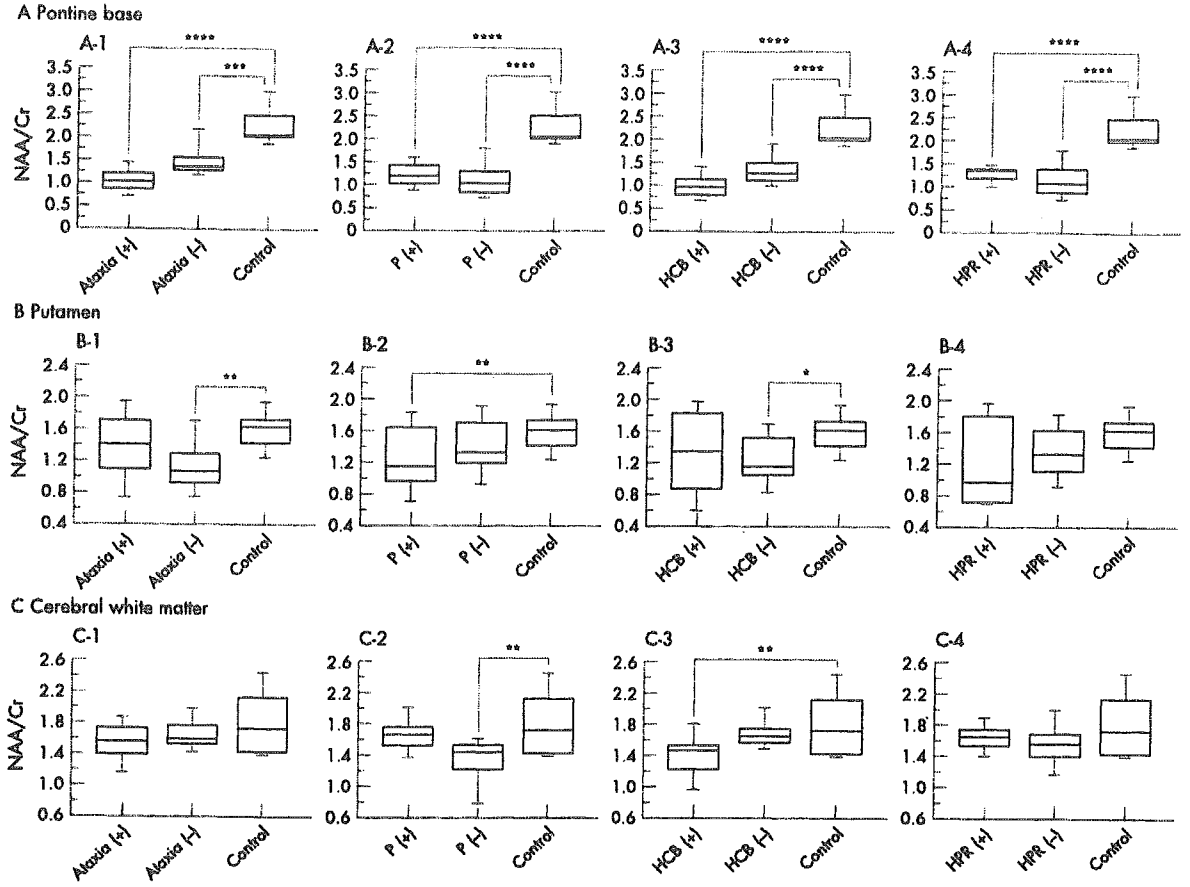

Figure 5 NAA/Cr in the pontine base (A), putamen (B) , and cerebral white matter (C) for MSA patients classified in terms of clinical features of ataxia (+ or −; A-1, B-1, C-1), parkinsonism (P; + or −; A-2, B-2, C-2), HCB on MRI (+ or −; A-3, B-3, C-3), and hyperintense putaminal rim (HPR) on MRI (+ or −; A-4, B-4, C-4). +, Presence; −, absence. *p = 0.047, **p = 0.02, ***p = 0.0006, and ****p<0.0001 by Scheffé's test, respectively. NAA, N-acetylaspartate; Cr, creatine; MSA, multiple system atrophy; CWM, cerebral white matter.

in the pons would be more extensive than in the putamen. As the pontine base consists of the axons and neurones specifically involved in MSA (for example fibres of cerebellar inflow and outflow, corticospinal tracts and transverse pontine tracts), subclinical involvement of such fibres could be detected as a reduction of NAA/Cr. Furthermore, because, as we demonstrated previously, MSA-C is significantly more prevalent in Japan than MSA-P, compared with white populations in the western countries,[7] the cerebellar pontine system should be more profoundly involved in Japanese MSA patients. A second possibility is that the volume effect due to putaminal atrophy would ultimately include the neighbouring normal tissues in the VOI of the MRS, influencing the degree of the NAA/Cr reduction. As atrophy of the putamen is severe in certain patients, the size of the VOI is a limiting factor in ^{1}H-MRS for maintaining an acceptable SNR. Such volume effects due to putaminal atrophy can result in conflicting data. Clarke and Lowry reported an absence of significant reductions in basal ganglionic NAA/Cr in MSA,[16] precluding the use of NAA/Cr reductions in the striatum for differential diagnosis.[18] Disease duration in their patients averaged 7.9 years.[16] In contrast, mean disease duration in other reports showing significant NAA/Cr reductions in the striatum of MSA patients ranged from 3.2 to 4.5 years,[11-14] similar to the duration in our patients. Because, with longer duration, putaminal atrophy in patients with MSA-P becomes more severe, discrepancies could be explained by differences in putaminal atrophy that can profoundly influence ^{1}H-MRS results. By avoiding this volume effect, MRS for the pontine base would provide a more accurate diagnostic marker.

Discriminating clearly between MSA-P and PD has long been a diagnostic problem from both therapeutic and prognostic viewpoints. Putaminal NAA/Cr reduction was significant in MSA-P patients compared with PD and control subjects, as previously reported.[11-14] However, as discussed above, the putaminal volume effect could influence the significance of putaminal NAA/Cr reduction, particularly in patients with advanced disease. Although brainstem and cerebellar involvement is an important and specific finding in differentiating MSA-P from PD,[26 32] the sensitivity of both clinical and MRI evaluations of these abnormalities is relatively low.[7 26] Based on our results, we believe that ^{1}H-MRS assessment of the pontine base would be of considerable value in the differential diagnosis between MSA-P and PD. However, combined ^{1}H-MRS study of the pontine base and putamen can provide a more sensitive differentiation between MSA-P and PD than a conventional single regional study, such as that of the putamen.

The cerebral hemisphere is involved more extensively in MSA than previously believed. Recently, Abe *et al* reported a significant decrease in NAA/Cr in MSA, involving Brodmann's areas 6, 8, and 46.[14] Moreover, Spargo *et al*

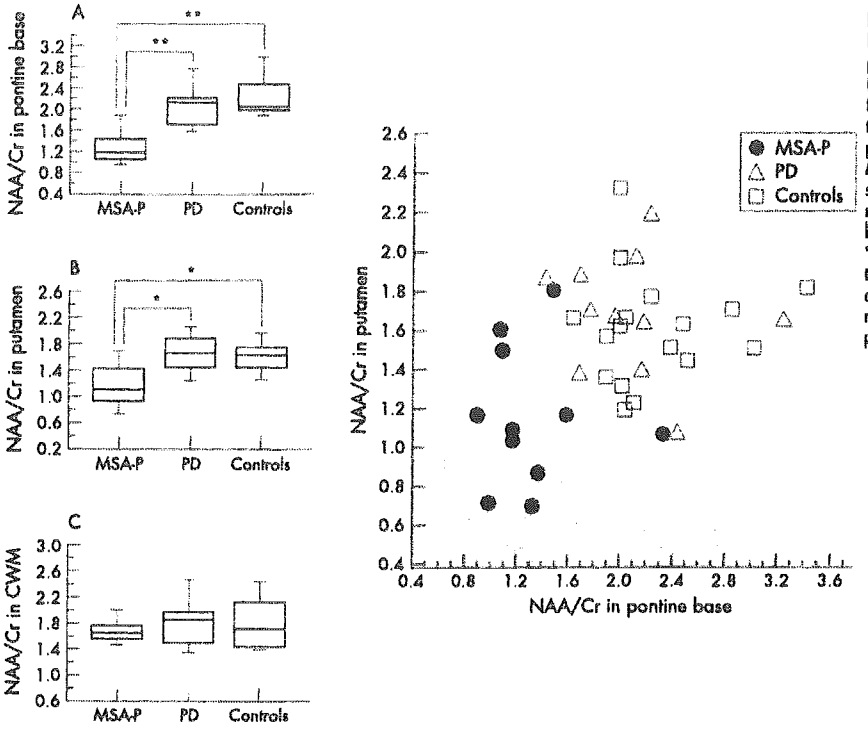

Figure 6 Box and whisker plot of the NAA/Cr ratio in the pontine base (A), putamen (B) and cerebral white matter (CWM, C) compared between MSA-P, PD, and controls. D is a scatter plot of the individual NAA/Cr data in the pontine base *v* putamen including MSA-P, PD, and control subjects. The scaled area corresponds to the mean−2 SD of NAA/Cr in the pontine base and putamen of control subjects. *p = 0.002, **p<0.0001 by Scheffé's test, respectively. NAA, *N*-acetylaspartate; Cr, creatine; MSA-P, multiple system atrophy with parkinsonism predominant.

reported 18.7% and 21.4% neuronal loss in the primary and supplementary motor cortex, respectively.[33] In addition, the degree of atrophy in cerebral hemispheric areas varies between individuals, often becoming severe in long standing cases.[34] We found a mild overall reduction of NAA/Cr in CWM with a more significant NAA/Cr reduction in the subgroup with a longer duration of illness. This finding is in good agreement with previous ^{1}H-MRS reports and pathological observations.

Davie *et al*[11] reported a significant reduction of Cho/Cr ratio suggesting reduced membrane turnover in the lentiform nucleus in MSA, perhaps as result of cell loss. In the present study, Cho/Cr showed little change throughout the course of disease in the putamen, pontine base, and CWM, in agreement with other reports.[12–16 18] The relevance of this discrepancy is uncertain. One possible explanation is the difference of technical factors such as size of VOI and echo time. On the other hand, pathological study shows not only cell loss but also widely and variously distributed myelin degeneration in MSA brains that may increase the Cho.[33] Thus, heterogeneity of lesions in association with disease stage also may influence the Cho/Cr result. Further longitudinal studies and comparison of ^{1}H-MRS with histological findings will be needed to clarify the uncertainty as to the Cho/Cr ratio in MSA.

In conclusion, localised ^{1}H-MRS at 3.0 T in multiple regions showed widespread neuronal and axonal involvement in patients with MSA. NAA/Cr reduction in the pontine base provided a significant diagnostic marker for MSA irrespective of the disease form of MSA-P or MSA-C, disease duration, symptomatic manifestations, or MRI abnormalities. Moreover, combined ^{1}H-MRS study of the pontine base and putamen proved particularly effective in differentiating MSA from PD. We believe that ^{1}H-MRS would provide an early and accurate MSA diagnosis, an enhanced understanding of its pathogenetic mechanism, and the conclusiveness needed for future therapeutic trials.

Authors' affiliations
H Watanabe, M Katsuno, M Sugiura, K Hamada, Y Okada, M Hirayama, G Sobue, Department of Neurology, Nagoya University Graduate School of Medicine, Japan
H Fukatsu, T Ishigaki, Department of Radiology, Nagoya University Graduate School of Medicine, Japan

Competing interest: none declared

REFERENCES

1 **Graham JG,** Oppenheimer DR. Orthostatic hypotension and nicotine sensitivity in a case of multiple system atrophy. *J Neurol Neurosurg Psychiatry* 1969;**32**:28–34.
2 **Quinn N.** Multiple system atrophy–the nature of the beast. *J Neurol Neurosurg Psychiatry* 1989;**52**:78–89.
3 **Gilman S,** Low PA, Quinn N, *et al.* Consensus statement on the diagnosis of multiple system atrophy. *J Neurol Sci* 1999;**163**:94–8.
4 **Sobue G,** Terao S, Kachi T, *et al.* Somatic motor efferents in multiple system atrophy with autonomic failure: a clinico-pathological study. *J Neurol Sci* 1992;**112**:113–25.
5 **Wenning GK,** Ben-Shlomo Y, Magalhes M, *et al.* Clinicopathological study of 35 cases of multiple system atrophy. *J Neurol Neurosurg Psychiatry* 1995;**58**:160–6.
6 **Lantos P.** The definition of multiple system atrophy: A review of recent developments. *J Neuropathol Exp Neurol* 1998;**57**:1099–111.
7 **Watanabe H,** Saito Y, Terao S, *et al.* Progression and prognosis in multiple system atrophy; an analysis of 230 Japanese patients. *Brain* 2002;**125**:1070–83.
8 **Ross B,** Michaelis T. Clinical applications of magnetic resonance spectroscopy. *Magn Reson Q* 1994;**10**:191–247.
9 **Davie CA.** The role of spectroscopy in parkinsonism. *Mov Disord* 1998;**13**:2–4.
10 **Rudkin TM,** Arnold DL. Proton magnetic spectroscopy for the diagnosis and management of cerebral disorders. *Arch Neurol* 1999;**56**:919–26.
11 **Davie CA,** Wenning GK, Barker GJ, *et al.* Differentiation of multiple system atrophy from idiopathic Parkinson's disease using proton magnetic resonance spectroscopy. *Ann Neurol* 1995;**37**:204–10.
12 **Federico F,** Simone IL, Lucivero V, *et al.* Proton magnetic resonance spectroscopy in Parkinson's disease and atypical parkinsonian disorders. *Mov Disord* 1997;**12**:903–9.
13 **Federico F,** Simone IL, Lucivero V, *et al.* Usefulness of proton magnetic resonance spectroscopy in differentiating parkinsonian syndromes. *Ital J Neurol Sci* 1999;**20**:223–9.
14 **Abe K,** Terakawa H, Takanashi M, *et al.* Proton magnetic resonance spectroscopy of patients with parkinsonism. *Brain Res Bull* 2000;**52**:589–95.